

LONG TERM BEHAVIOR OF ACID FORMING ROCK: RESULTS OF 11-YEAR FIELD STUDIES¹

PAUL F. ZIEMKIEWICZ² and F. ALLEN MEEK JR.³

Abstract: The ability to predict long term acid mine drainage (AMD) under field conditions is limited by the near absence of long-term, well controlled and well documented field sites. Much of the literature on AMD derives from either uncontrolled, operational mine sites or from laboratory studies using a variety of simulated weathering methods.

In February 1982, Island Creek Corporation constructed eleven 400 ton rock piles on plastic lined pads at its Upshur County, WV coal mine. The piles ranged from 100% sandstone to 100% shale with several mixtures of the two rock types. Leachate waters were collected biweekly during the first year and subjected to chemical analysis. Because water volumes were also measured it was possible to estimate mass balances and flux rates for key constituents such as sulfur, calcium and acidity.

Eleven years after construction the piles were again sampled. Data are presented indicating the rates of sulfur flux from each of the piles and changes in water quality over the 11 years of the study. Of particular interest was the tendency of the sulfur flux rate to approximate that reported for pure pyrite under laboratory conditions.

Additional Key Words: Acid mine drainage, coal spoil, alkaline amendment.

Background

Acid Base Accounting.

Acid Base Accounting (ABA) was developed in the early 1970's by researchers at West Virginia University to identify and classify geologic strata encountered during mining (West Virginia University, 1971). A history of Acid Base Account is provided by Skousen et al. (1990).

Since its development, ABA has been used extensively in the United States and several other countries for premining coal overburden analysis. Its popularity largely stems from its simplicity. It uses two key parameters: maximum potential acidity (MPA) and neutralization potential (NP). MPA is estimated by multiplying the percent pyrite sulfur by 3.125 yielding the total acid produced. NP is the acid consumed by the rock in a titration. Both MPA and NP are given in calcium carbonate equivalents. ABA does not address the different rates of acid and alkali-generating reactions in rock.

Introduction

The long term behavior of acid producing rock under field conditions has been the subject of much speculation and modelling but relatively little systematic study.

DiPretoro and Rauch (1988) found poor correlations (reported $R^2=0.16$) between a volume-weighted acid base net neutralization potential (NP) and net drainage alkalinity near thirty mine sites in West Virginia. Erickson and Hedin (1988) showed similar low correlation among MPA, NP, net NP from ABA and net alkalinity from drainage

¹ Paper presented at the International Land Reclamation and Mine Drainage Conference and the Third International Conference on the Abatement of Acidic Drainage, Pittsburgh, PA, April 24-29, 1994.

² Director, National Mine Land Reclamation Center, West Virginia University, Morgantown, WV, USA.

³ Glen Springs Holding Company, Lexington, KY, USA.

water. Both reports related that factors other than overburden characteristics were involved in predicting post mining water quality.

DiPretoro and Rauch (1988) found that sites with greater than 3% calcium carbonate equivalent (NP) in overburden produced alkaline drainages while at 1% or less acidic drainage resulted. Erickson and Hedin's results indicate that 2% calcium carbonate or less produced acidic drainage while 8% or more produced alkaline drainage. (In this later study there were no sampling points between 2% and 8%).

O'Hagan and Caruccio (1986) found that the addition of calcium carbonate at 5% by weight to a coal refuse containing 1% S produced alkaline drainage. In Minnesota, Lapakko (1988) found that 3% calcium carbonate neutralized an overburden material with 1.17% S.

Cravotta et al. (1990) reviewed the calculation of NP in ABA. In current ABA usage, 3.125 g calcium carbonate equivalent is required to neutralize acidity resulting from oxidation of 1 g S. Cravotta et al. (1990) argue that this ratio should double to 6.25:1. Volume-weighted maximum acidities are subtracted from NP giving a positive or negative net NP for the mined area. A negative, or deficient, net NP is interpreted to indicate the amount of calcite that must be added to equalize the deficiency and prevent AMD formation.

Other alkaline materials have higher NP's than calcite. Quicklime, kiln dust and hydrated lime all have higher activities than calcite, though it is not clear that the kinetics of pyrite oxidation favor readily soluble sources of alkalinity.

Brady et al. (1990) conducted a study of 12 sites where ABA data were available. They computed net NP based on both 3.125% and 6.25% to 1% S. Alkaline addition on the sites was conducted to abate potential AMD problems. When using 6.25%, the sign of the net NP (plus or minus) matched the sign of the overall net alkalinity of water at 11 of 12 sites.

The results of their study concluded that NP and traditional estimates of MPA (e.g. 3.125% to 1% S) were not equivalent and that overburden NP must be twice the MPA to produce alkaline mine drainage. They also concluded that mining practices (such as alkaline addition, selective handling, and concurrent reclamation) enhanced the effect of alkaline addition on reducing acidity. Lastly, they concluded that additional studies are needed to determine the rates, application and placement of alkaline material during mining.

Methods

Island Creek Corporation constructed a series of 11 test piles at its Upshur County, WV mining complex between January and March 1982. Rocks used in the trials were taken from the company's active mining operations on the site and were sized to exclude roughly +8 in. and -1 in. rocks. Treatments consisted of various combinations of sandstone and shale. Another series of treatments consisted of various amendments for controlling AMD.

About 400 tons of rock were placed in each test pile. Each rock mass was placed on a plastic liner with an 8 inch perforated pipe for collection of drainage to an automatic sampling station. The piles were flat-topped and were roughly 16m X 16m X 2m. The rock units were sampled on placement in each pile and ABA were developed for each. Table 1 describes the treatments and properties of each pile. Treatments can be summarized thus:

Table 1. Identification, summary of treatments and NP/MPA of the 11 test piles, Upshur County, WV.

<u>PILE #</u>	<u>DESCRIPTION</u>	<u>CODE</u>	<u>NP/MPA</u>
CONTROL, NO AMENDMENT			
PILE 1	100% sandstone	SS	3.94
2	100% shale	SH	0.08
3	sandstone/shale in layers	LAY	0.18
10	sandstone/shale blended	BLD	0.29
LIMESTONE AMENDMENT			
PILE 5	0.5% by mass	LS1	0.46
4	1.65% by mass	LS2	1.07
8	2.4% by mass	LS3	1.26
PHOSPHATE AMENDMENT			
PILE 7	0.15% by mass	RP1	0.15
6	0.3% by mass	RP2	0.31
CALCIUM OXIDE AMENDMENT			
PILE 9	0.62% by mass	CaO	0.15
BACTERICIDE AMENDMENT			
PILE 11	30 lbs. sodium lauryl sulfate +31 lbs Microwet #2 + impregnated pellets	SLS	0.41

Amendments were spread over one foot spoil layers during construction. A rain gauge was maintained on the site during the period of the study. Annual precipitation averaged 45 inches. The pH of the local rainfall averaged about 4.5.

Immediately following pile construction, water samples were collected and analyzed weekly, then later bi-weekly for roughly the first year. Sampling then halted for the next 11 years until January 1993. The following parameters were measured: flow, acidity, alkalinity, pH, sulfate, calcium, magnesium, iron and manganese. Since flow was measured it was possible to develop mass balances for various ions, particularly sulfate.

With the exception of pile 1 all of the piles were undisturbed when sampled in January 1993. About one half of pile 1 had been excavated and could not be sampled. The automatic samplers had been removed from each pile and it was not possible to estimate flows. Therefore, only chemical concentrations are reported for the January 1993 sample. Flow data were based on flow meters attached to the outlet of each pile. They did not always work and some of the flow data is inferential (e.g. calibrated against precipitation). Nonetheless, it was clear that flows varied little among piles at a given time interval.

A key parameter in developing the sulfur dynamics was sulfur flux (Sf). Sulfur flux was expressed as the percent of the original pyrite sulfur mass which had exited the pile as sulfate ion. Sulfur flux integrates both pyrite oxidation and sulfate leaching rates into a single, empirical parameter.

Results

The results are based on 400 ton test piles constructed in mid-winter 1982. Only one sample was taken of each rock unit during placement so that on a given pile NP and MPA are based on a one shale sample and/or one

sandstone. It is likely that the distribution of pyrite and alkalinity were neither homogeneous nor random and that reported NP/MPA ratios may be subject to error. It is also possible that the placement of alkaline amendments was not uniform. Results of the sampling program are presented in figures 1-6. Treatments are summarized in table 1.

Control, No Amendment. In piles SS and SH pH fell rapidly to about 4.2 over the first 7 months while sulfate rose from near zero to the range 2000 to 2500 ppm. Leachate sulfate concentrations from LAY and BLD rose to about 2700 ppm while pH fell less dramatically to 4.9 and 6.2 respectively. By January 1993, pH had changed little while sulfate concentrations dropped to less than 100 ppm. At least over the first year, blending seemed to improve the pH of the piles while there appeared to be little effect on sulfate generation. See figures 1 and 2.

Limestone Amendment. Addition of limestone had no effect on the rate of sulfate generation and, by inference, the rate of pyrite oxidation. Over the first year, the pH of LS1 AND LS2 remained above neutral while LS3 became acid. Nonetheless, 11 years later the final pH of LS1, LS2 AND LS3 were 5.2, 6.4 and 6.6 respectively. It is not clear why LS3, with the highest NP/MPA initially became acid. Sulfate generation was the same as the other piles so the difference must lie in the efficiency with which the available alkalinity was utilized. This could be a result of initial placing and mixing but records indicate no compelling cause for this result. It is also not clear how long LS3 remained acid. By year 11, at any rate, it had the highest pH.

Sulfate generation was the same as the control piles (SS, SH, LAY, BLD) and by year 1 sulfate concentrations had dropped to below 350 ppm. See figures 3 and 4.

Phosphate Amendment. Sulfate profiles of the two phosphate treatments over the 11 years of the study indicate that pyrite oxidation is not affected by phosphate addition. Effluent pH remained above or near neutral for the first year. The pH of RP1 AND RP2 then dropped to 4.7 and 3.8 respectively. It is not clear why the heavier phosphate application reached a lower pH or whether the difference is even significant. It is clear that phosphate does not control pyrite oxidation, but simply acts as a lime by neutralizing produced acidity. Mindful that it is usually much more expensive than limestone, it should if used, be applied at rates similar to those at which limestone is effective. See figures 5 and 6.

Calcium Oxide Amendment. Sulfate concentrations, like all of the other plots rose rapidly over the first 7 months of the study, reached a peak of about 2500. By year 11 sulfate concentration on this pile was less than 100 ppm. Over this period pH declined rapidly, and by year 11 was about 4.2, the pH of the local rainwater. See figures 5 and 6.

Bactericide Amendment. Sodium lauryl sulfate is a bactericide, meant to control the rate of pyrite oxidation by killing the *Thiobacillus ferroxidans* bacteria. The sulfate concentration profile for this treatment suggests that pyrite oxidation was little affected by the treatment and that the primary effect of the treatment was to increase the pH over the first year. By year 11 pH was about 4.2. The pH and sulfate profiles are consistent with an alkaline amendment applied at less than adequate rates. See figures 5 and 6.

Sulfur Flux. Sulfur flux through each pile ranged from 0.064% per day to slightly less than 0.01% per day. With only two exceptions all values fell between 0.01% and 0.03% per day (figure 7). For comparison, the literature value of Taylor et al. (1984) of 0.02% per day is presented. This is a surprising level of agreement given the inherent errors expected in estimating original pyrite sulfur contents of the rock masses.

When the results were ranked according to sandstone content (figure 8) it was apparent that sulfur flux is strongly influenced by the proportion of sandstone. Sulfur flux took about nine months to reach its maximum observed rate. Figures 9 and 10 indicate the acceleration of sulfur flux in selected piles.

Figure 1. LEACHATE pH-UNTREATED PILES

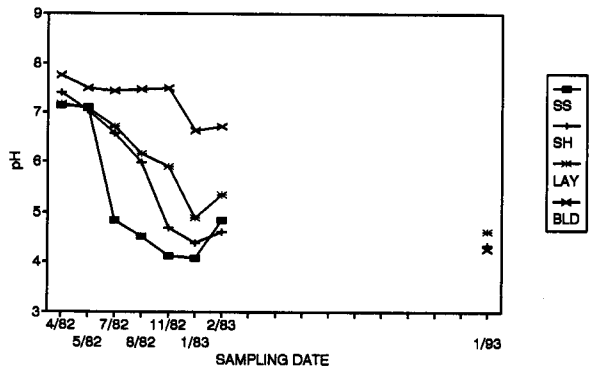


Figure 2. LEACHATE SULFATE (PPM) UNTREATED PILES

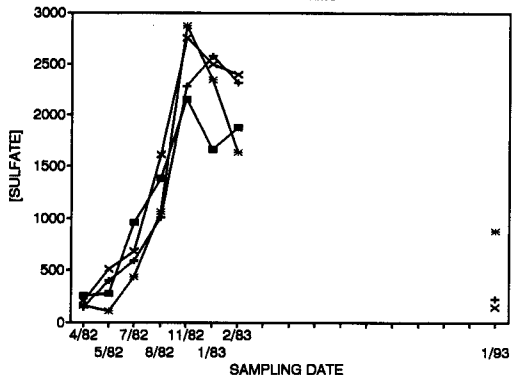


Figure 3. LEACHATE pH-LIMESTONE TREATED PILES

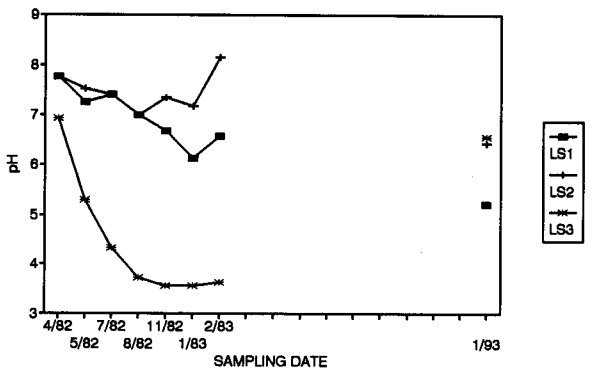


Figure 4. LEACHATE SULFATE (PPM) -LIMESTONE TREATED PILES

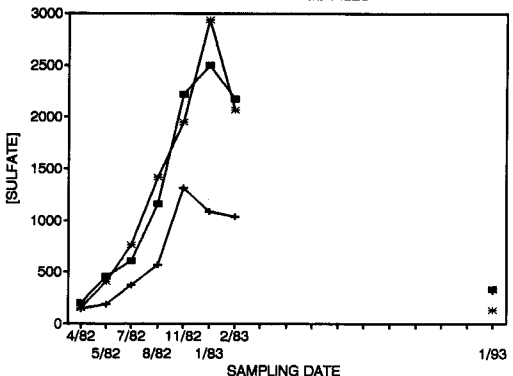


Figure 5. LEACHATE pH-PHOSPHATE, CaO, SLS TREATED PILES

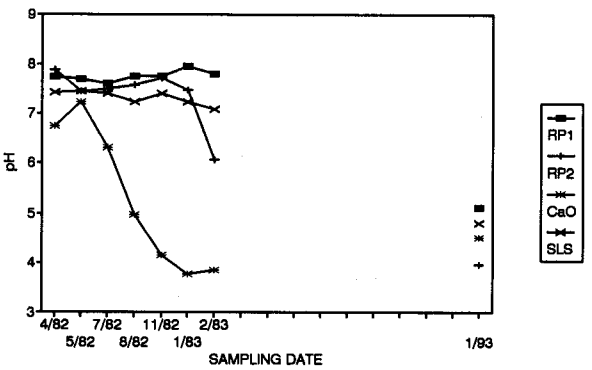


Figure 6. LEACHATE SULFATE (PPM) -PHOSPHATE, CaO, SLS TREATED PILES

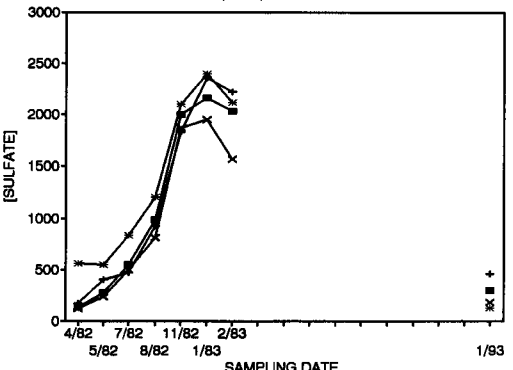


Figure 7. SULFUR LOSS RATES FROM THE 11 TEST PILES AND A LITERATURE VALUE (LIT)

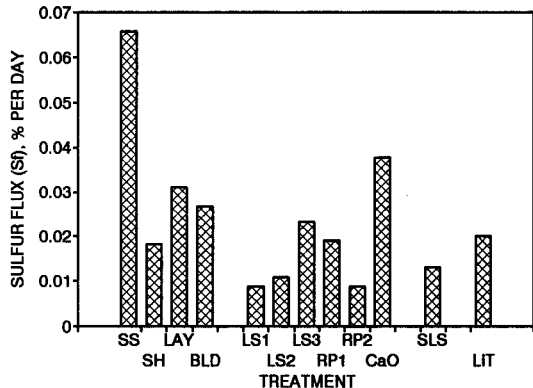


Figure 8. SULFUR LOSS RATES FROM THE 11 PILES RANKED BY SANDSTONE CONTENT

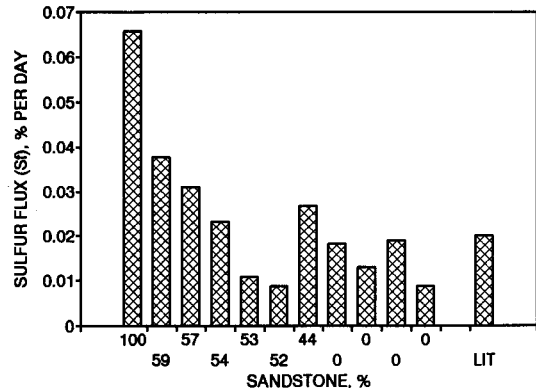


Figure 9. CHANGE IN SULFUR FLUX DURING THE FIRST YEAR, UNAMENDED PILES

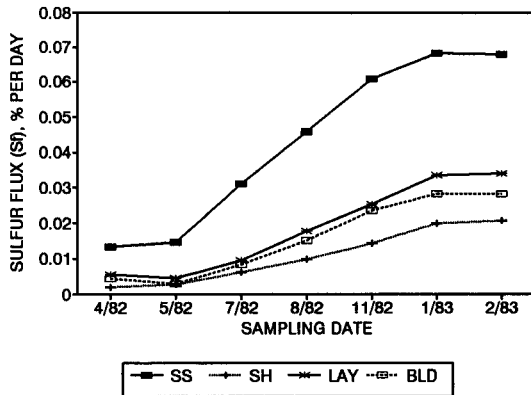
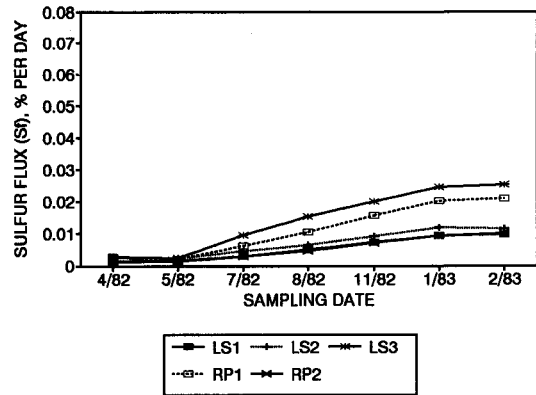


Figure 10. CHANGE IN SULFUR FLUX RATES DURING FIRST YEAR, AMENDED PILES



Conclusions

The following conclusions pertain to the results of observed leaching of eleven 400 ton piles of acid producing rock under field conditions in Upshur County, WV. The piles had a large surface area and were only 2 m thick. It is likely that leaching was optimized by this design and that storage was minimized. Sulfur flux rates would be much lower on a large, conventional rock dump. In the following discussion, therefore, sulfur flux is taken to estimate pyrite oxidation.

1. Pyrite oxidation in rock dumps is independent of overall leachate pH. While pH in the immediate vicinity of oxidizing pyrite grains would be low, circumneutral pore water pH will cause most metal ions to precipitate near the point of oxidation and the acidity to be quickly neutralized
2. At the rates tested in this trial pyrite oxidation was little affected by any of the following amendments: limestone, rock phosphate, calcium oxide and sodium lauryl sulfate.
3. There was no clear relationship between NP/MPA and pH performance of the piles. Since sulfate generation appeared to be consistent with estimated rock pyrite sulfur contents it is likely that substantial error occurred in the estimation of effective NP. The error could have had several causes: poor mixing of amendments and spoil types, inherent overestimation in the NP analysis procedure or sampling error.
4. It appears that gross physical phenomena, independent of pyrite forms, surface area, amendment, pH or micro properties of the rock control the rate of pyrite oxidation within relatively narrow limits. Since the rate increased with the proportion of sandstone, oxygen diffusion is the likely candidate.
5. In most, but not all cases, alkaline amendments tended to maintain a circumneutral pH over the first year while untreated piles quickly became acid.
6. In the two cases where limestone addition raised the NP/MPA above 1.65 a circumneutral pH was observed after 11 years. Untreated piles and those treated with rock phosphate, calcium oxide and SLS remained acid.

Literature Cited

- Brady, K., M.W. Smith, R.L. Beam and C.A. Cravotta. 1990. Effectiveness of the use of alkaline materials at surface coal mines in preventing or abating AMD: Part 2. Mine site case studies. pp. 227-241. In: Proceedings of the 1990 Mining and Reclamation Conference, West Virginia University, Morgantown, WV.
- Cravotta, C.A., K. Brady, M.W. Smith, and R.L. Beam. 1990. Effectiveness of the addition of alkaline materials at surface coal mines in preventing or abating AMD: Part I. Geochemical considerations. pp. 221-225. In: Proceedings of the 1990 Mining and Reclamation Conference. West Virginia University, Morgantown, WV.
- diPretoro, R.S. and H.W. Rauch. 1988. Use of acid-base accounts in premining prediction of acid drainage potential: a new approach from northern West Virginia. pp. 2-10. In: Mine Drainage and Surface Mine Reclamation. USDI Bureau of Mines Information Circular 9183.
- Erickson, P.M., and R.S. Hedin. 1988. Evaluation of overburden analytical methods as means to predict post-mining coal mine drainage quality. pp. 11-19. In: Mine Drainage and Surface Mine Reclamation. USDI Bureau of Mines Information Circular 9183.
- Lapakko, K. 1988. Prediction of AMD from Duluth Complex mining wastes in northeastern Minnesota. pp. 180-190. In: Mine Drainage and Surface Mine Reclamation. USDI Bureau of Mines Information Circular 9183.

O'Hagan, M., and F.T. Caruccio. 1986. The effect of admixed limestone on rates of pyrite oxidation in low, medium, and high sulfur rocks. In: 1986 National Symposium on Mining, Hydrology, Sedimentology, and Reclamation. University of Kentucky, Lexington, KY.

Skousen, J., R.M. Smith, and J. Sencindiver. 1990. Development of the Acid-Base Account. Green Lands 20(1): 32-37.

Taylor, B.E., M.C. Wheeler and D.K. Nordstrom. 1984. Stable isotope geochemistry of acid mine drainage: Experimental oxidation of pyrite. *Chemica et Cosmochimica Acta* Vol. 48. pp. 2669-2678. Pergamon Press Ltd.

West Virginia University. 1971. Mine spoil potentials for water quality and controlled erosion. 14010 EJE 12/71. Contract with West Virginia University by the U.S. Environmental Protection Agency, Washington, D.C.

SURFACE CHEMICAL METHODS OF FORMING HARDPAN IN PYRRHOTITE TAILINGS AND PREVENTION OF THE ACID MINE DRAINAGE¹

Syed M. Ahmed²

Abstract: This work was undertaken to identify conditions under which hardpan could be formed in pyrrhotite (FeS) rich tailings using surface chemical methods and to check the susceptibility of the synthetic hardpan to atmospheric oxidation and acid formation.

Pyrrhotite hardpan was first grown on a small scale (200 g) by surface chemical and electrochemical methods, after treating the FeS-rich tailings with a dilute solution of Fe^{2+} , pH adjustment, and curing for several weeks in the presence of air. This synthetic hardpan was similar to the phrrhotite hardpans formed under natural conditions, consisting of FeS grains embedded in iron oxyhydrate (goethite) matrix.

Attempts were then made to grow similar hardpans on a large scale with FeS columns of 3 ft length and 4 in diameter. The effects of surface oxidation of FeS in air, Fe^{2+} treatment, humidity, pH, and a water head (2 in) on the hardening of tailings and acid formation have been examined. Hardening was confined mainly to the outer layer of the tailings exposed to air; the inner core remained soft and retained most of the Fe^{2+} in the unoxidized form. The pH, dissolved iron concentration, and redox potentials of the percolant solutions were monitored. Most pronounced was the effect of maintaining 2 in of water head on the tailings, which prevented the oxidation of FeS and acid formation completely. The data have been examined in light of the Eh-pH diagram of the $\text{FeS}_2\text{-FeS-Fe}_2\text{O}_3$ system in equilibrium with water. It is inferred that the FeS system can be stabilized through formation of iron oxide and other less soluble compounds such as iron silicates on the surfaces. Methods of improving kinetics of hardpan formation have been suggested.

Additional Key Words: acid mine drainage, pyrrhotite, hardpan, sulfides.

Introduction

Natural formation of hardpans is often experienced in sulfide tailings that are exposed to air and water at the disposal sites. The hardpans normally consist of pyrrhotite (FeS) and pyrite (FeS_2) grains cemented in iron oxyhydrate (goethite) structure. This phenomenon has been attributed to the Fe^{2+} being oxidized to ferric oxyhydrates and forming hardpans in selective areas. Pyrite, being an electrocatalyst for oxygen reduction, undergoes little surface oxidation itself; hence pyrite hardpans are rare in nature.

In our earlier work (Ahmed and Giziewicz, 1992; Ahmed, 1990, 1991) in this field, the electrochemical and solid state properties of iron sulfides were examined, and the oxidative decomposition of iron sulfides was attributed to 'holes' or electron vacancies, formed as electrons are transferred from the substrate to oxygen or Fe^{3+} . The holes are electrically mobile and lead to bond breaking and decomposition. It was also reported that FeS and FeS_2 can be electrochemically passivated by growing iron oxide films on the sulfide surfaces. The oxide film would then protect the sulfide substrate from further oxidation. The Eh-pH diagram of the $\text{FeS-FeS}_2\text{-Fe}_2\text{O}_3$ system in equilibrium with water, as shown in fig. 1, indicates that iron sulfides under oxidizing conditions are unstable and produce acid and dissolved Fe^{2+} and Fe^{3+} . At sufficiently low pH, the dissolved Fe^{3+} in turn causes further oxidation and decomposition of the sulfides. The sulfide oxidation by air can occur even in a basic medium. On the contrary, iron oxides, being the oxidation products, can form a stable phase under oxidizing conditions as long as the medium is neutral or basic. Also, iron oxides can be further stabilized by converting the surface into less soluble compounds.

¹ Paper presented at the International Land Reclamation and Mine Drainage Conference and the Third International Conference on the Abatement of Acidic Drainage, Pittsburgh, PA, April 24-29, 1994.

² Research Scientist, Mineral Sciences Laboratories, CANMET, Natural Sciences, Canada, Ottawa, CANADA.

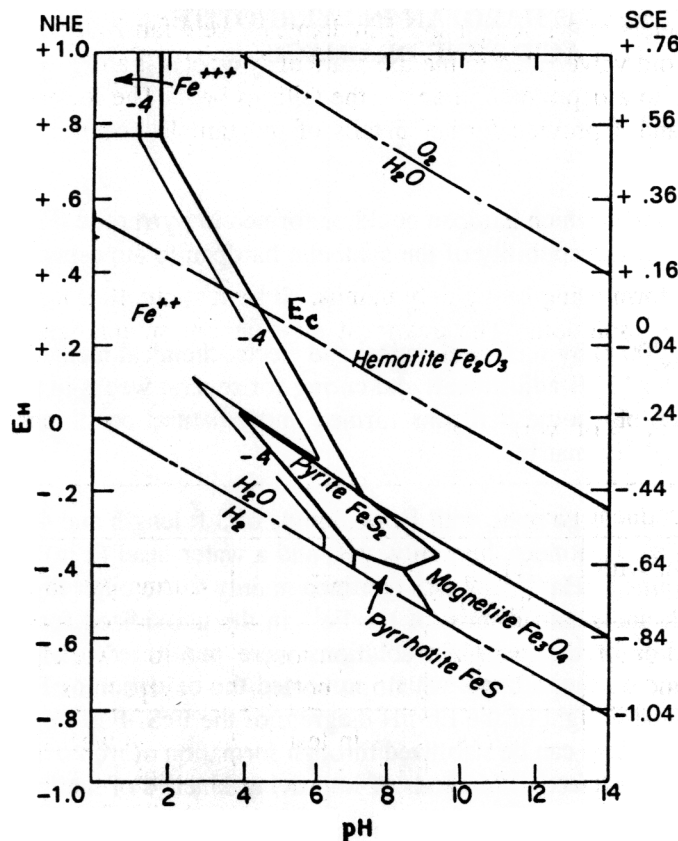


Figure 1. Eh-pH diagram showing the stability contours for pyrite, pyrrhotite and iron oxides in water at 25° C, when total S = 10^{-6} mol. Log of iron concentration is shown to be -4, the line indicating changes in solubility. The conduction band edge, E_c , of pyrite is also shown. The potentials relative to the saturated calomel electrode are shown on the right-hand side.

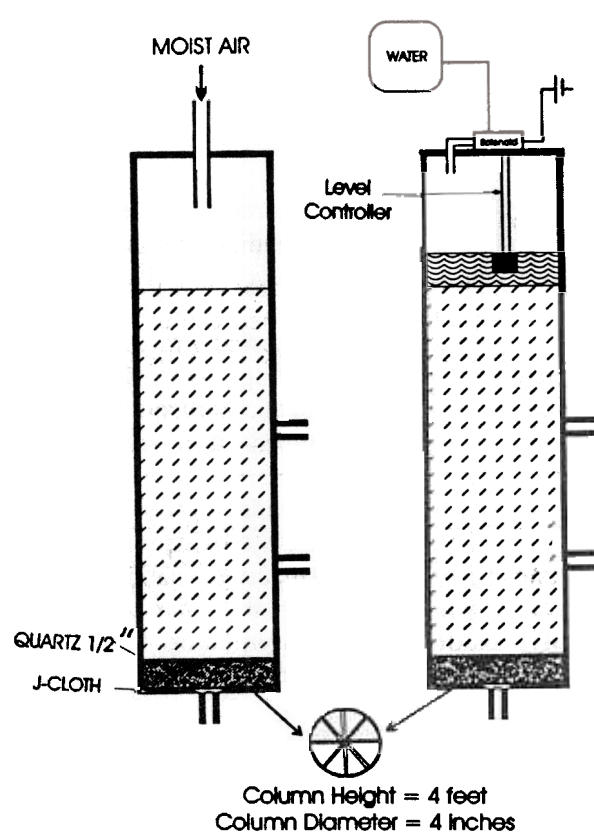
It follows from the foregoing considerations that it may be possible to control and even prevent the atmospheric oxidation of pyrrhotite and the resultant acid generation by converting the sulfide into an oxide hardpan where each FeS particle is coated with an iron oxide film and the particles cemented together to form a goethite structure.

The following work was therefore undertaken to examine the formation of pyrrhotite hardpans by surface chemical methods and to test their stability and susceptibility to atmospheric oxidation and acid formation.

Experimental Methods

Materials and Equipment

Fresh pyrrhotite tailings in unoxidized form were obtained from the Sudbury (Ontario) area. From image analyses, these tailings were found to contain 78% pyrrhotite, 15% magnetite, 4% silicates, and 3% chalcopyrite, pentlandite, and other minor constituents. The tailings were first oxidized in a slurry form by bubbling air through the slurry for 12 h. These samples are henceforth referred to as "laboratory oxidized" tailings. Another batch of fresh tailings was exposed to air in a steel tray for two weeks in moist condition at room temperature. The tailings were raked frequently for uniform oxidation. These samples are referred to as 'naturally oxidized' tailings in the text to follow.



For large-scale experiments, five cylindrical lysimeters of 4 ft length and 4 in diameter were fabricated from clear plexiglass of 1/8 in wall thickness (fig. 2). A solenoid valve fitted to the top plate of lysimeter 2 and a water reservoir enabled control of the water level automatically to a depth of 2 in above the tailings bed. The following is a detailed description of the procedures. Figures 3 and 4 provide further details of the sample histories and treatment.

Oxidation and Loading

The lysimeters were loaded with tailings in slurry form using heavy duty pumps. It took about 48 h for the tailings to settle before the bed could be treated with Fe^{2+} solution. The treatment methods are summarized in table 1 in sequential form and are further described below.

Table 1 - Summary of work

Lysimeter	Treatment method					
	Tailings type	Laboratory oxidation	Treatment with Fe^{2+}	Curing period 1	pH	Curing period 2
1	Fresh, unoxidized	Yes	Soak and drain method	2 weeks	8.5 on top, 5.5 at bottom	6 to 8 weeks, kept moist
2	Fresh, unoxidized	Yes	Percolation	2 weeks	as in test 1	6 to 8 weeks, kept 2.5 cm solution head
3	Naturally oxidized	No	Soak and drain method	2 weeks	as in test 1	6 to 8 weeks, kept moist
4	As in test 1, without Fe^{2+} treatment					
5	Fresh unoxidized	Yes	Intimate mixing	2 weeks	as in test 1	Air

Treatment with Fe^{2+} Solution

Lysimeters 1, 3, and 4 were treated with a 0.01M solution of Fe^{2+} (2.78 g/L of $\text{FeSO}_4 \cdot 7\text{H}_2\text{O}$) at a pH ~ 6, by a "soak and drain method" in which the column was first soaked with a solution head and then allowed to drain naturally until the percolant solution contained at least 0.001M of the ferrous salt. In the case of lysimeter 2, the Fe^{2+} solution was percolated from the top until the percolated solution at the bottom had acquired the required concentration (~ 0.001M) of ferrous salt. In the case of lysimeter 5, however, the tailings were intimately premixed with the Fe^{2+} solution in the drum itself before being transferred to the lysimeter. Lysimeter 4 was set up for a blank run without any treatment with the ferrous solution.

Tailings in lysimeter 2 were maintained under a constant head of water as described earlier, while column 5 was kept exposed to air under natural, atmospheric conditions.

Curing Period 1

After treatment with ferrous salt, the columns were left for an initial period of 2 weeks of curing to allow oxidation of ferrous to ferric iron take place under moist conditions. Extra moisture was maintained in lysimeters 1, 3, and 4 by bubbling air through water aspirators and circulating the moist air on the top of the tailings.

After 2 weeks of curing (period 1), tap water adjusted to a pH of 10.5 was allowed to percolate through the tailings until the percolant solution had reached a pH of at least 6. A pH of 6 was selected because the zero point of charge of iron oxides lies between pH 5.5 and 6.5, at which the solubility of iron oxides is minimum. Also $\text{Fe(OH)}_3\text{-Fe}_2\text{O}_3$ starts precipitating at about this pH. The tailings were then left for a curing period of 8 to 10 weeks for the hardpan to form.

Since water in lysimeter 2 was kept under constant flowing conditions, the percolant solution in this case was monitored continuously during the 8 week period for pH, Eh, and dissolved iron concentration. The results obtained for all lysimeters at the beginning and at the end of the curing periods are presented in graphical form in figures 3 and 4, respectively.

Small Scale Experiments

Hardpans were grown by both surface chemical and electrochemical methods using 200 g samples of fresh pyrrhotite tailings in each test. In the former case, samples with and without being surface oxidized were subjected to surface chemical treatment separately in glass tubes of 1 in diameter. The rest of the treatment was the same as in lysimeter 5.

In the second method, the tailings were subjected to cathodic treatment in K_2SO_4 solution using a two compartment cell with a fritt glass junction. A graphite rod immersed in the tailings bed served as the cathode and an inert metal electrode was used as anode. A potential of -200 to -300 mV (SCE) was applied potentiostatically with a current of ~0.1 mA passing through the cell under steady state conditions. Further details may be seen elsewhere (Ahmed, 1991).

Results and Discussion

Small Scale Experiments

The electrochemically treated tailings (no Fe^{2+} added) and tailings treated with Fe^{2+} after oxidation with air hardened in about 6 weeks. The glass walls broke at this stage, most probably due to cementing of the iron oxide in the hardpan with the glass walls and subsequent contraction. No such breakage of walls occurred in plexiglass but shrinkage from the walls was observed. Fresh tailings treated with Fe^{2+} , without any surface oxidation, took longer to harden.

The hardpans from these experiments were examined by scanning electron microscopy. The backscattered electron image (BEI) and hardpan photographs are shown in figures 5 to 8. It is seen in figures 6, 7, and 8 that the FeS-FeS_2 grains in these hardpans are cemented in a goethite (+ lepidocrocite) structure and that the synthetic and natural hardpans of pyrrhotite have the same structure (figs. 7,8). The pyrite hardpan (fig. 6), however, is seen to be separated from the goethite phase by a third phase which seems to be a dehydrated form of iron oxide.

Lysimeter Tests

Probe tests with nails after the second curing period indicated that the hardening of tailings was confined mainly to the outer layer of the beds exposed to air; the inner core, which was not exposed to air (oxygen), remained soft and retained most of the Fe^{2+} in the unoxidized form. Obviously, the Fe^{2+} in the inner core of the tailings was not oxidized and not precipitated as ferric oxyhydrate. As a result, the excess of Fe^{2+} (~0.001M) drained out through columns 1, 3, 4, and 5 during percolation tests, as shown in fig. 4. The pH of the percolant solutions was between 5 and 6.

HISTORY		Redox Potentials
April 2	Tailings loaded	Fe^{2+} Soln. = 0.243 V
April 6	Initial settling	
April 8	Solution clearing	#5 = 0.046 V (SCE)
	Fe^{2+} Addition started	#2 = 0.120 V (SCE)
April 29	Fe^{2+} Addition ended	#1 = 0.186 V (SCE)
May 4	pH adjusted; $\text{pH}_i = 10.45$	
May 29	Fe^{2+} added to lysmtr. #3	

Flow Rates:
0.7 to 0.8 mL/mm

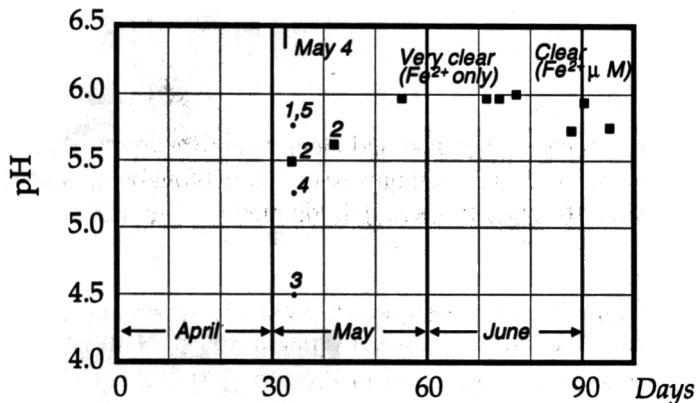


Figure 3. Diagram showing the history and a record of redox potentials, pH and Fe^{2+} concentration in the percolating solution, during the first 3 months. The numbers refer to different lysimeters and ● ■ refer to readings for respective lysimeters.

HISTORY

Aug 28, 1993
Lysimeter 1,2,3,4 and 5 filled with water & percolation tests carried out.

Redox Potentials :-

# 1	0.0640	V (SCE)
# 2	- 0.0230	V (SCE)
# 3	0.0834	V (SCE)
# 4	0.0653	V (SCE)
# 4X	0.1236	V (SCE)
# 5	0.0692	V (SCE)

FLOW RATES

#2	Uniform	1.07 mL/min
#1	Fast	27 mL/min
	Slow	0.18 mL/min
#3	Slow	0.26 mL/min
#5	Fast	33 mL/min
	Slow	0.6 mL/min

Fast and slow refer to flow rates through the annular space (between column and lysimeter wall) and through the tailings column, respectively.

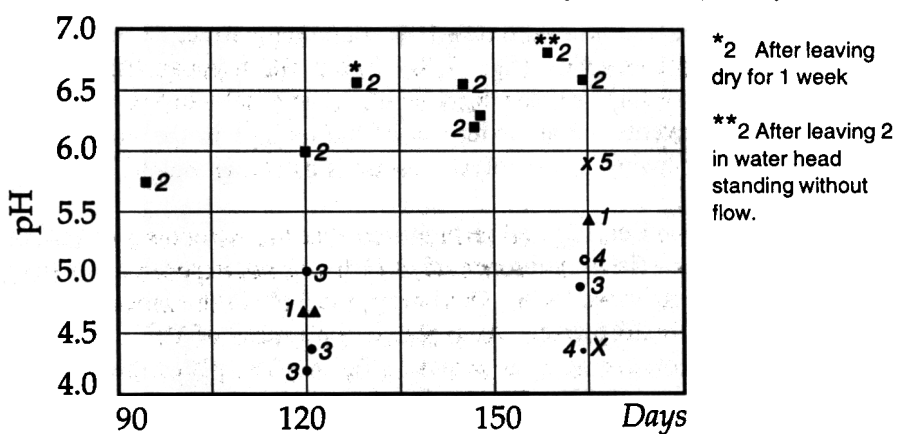


Figure 4. Diagram showing the history and a record of redox potentials, pH and Fe^{2+} concentration in the percolating solution, during the last 3 months. The numbers refer to different lysimeters ● ■ refer to readings for respective lysimeters.

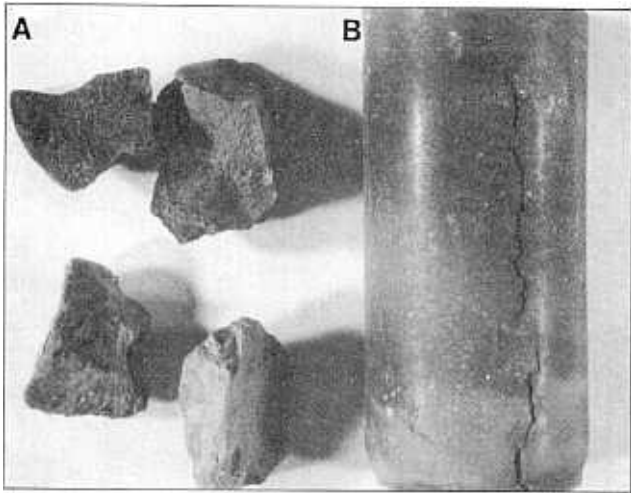


Figure 5A. Surface chemically formed pyrrhotite hardpan, obtained after a preoxidation step (pieces shown);

Figure 5B. Surface chemically formed pyrrhotite hardpan obtained without any pre-oxidation.

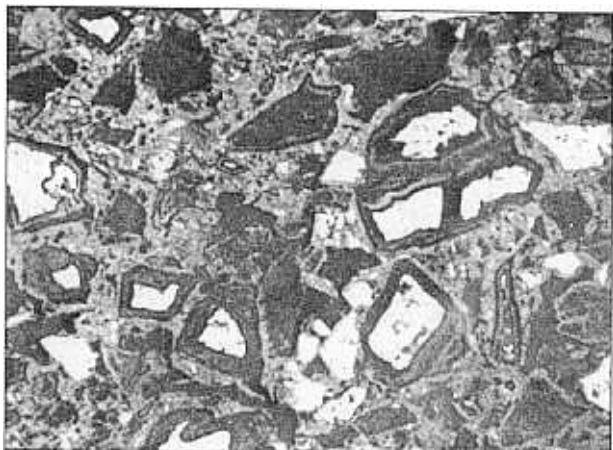


Figure 6. BEI photographs of natural, pyrite hardpan showing FeS_2 grains (white) coated with an iron oxide film, embedded in goethite matrix.

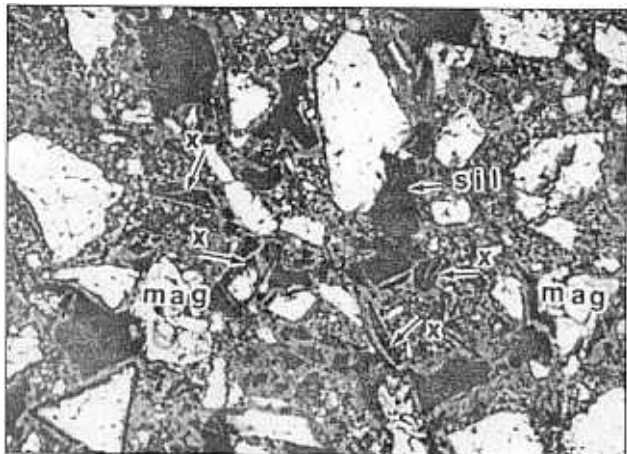


Figure 7. Synthetic hardpan showing pyrrhotite grains embedded in goethite matrix (+ some magnetite). White grains -- FeS .

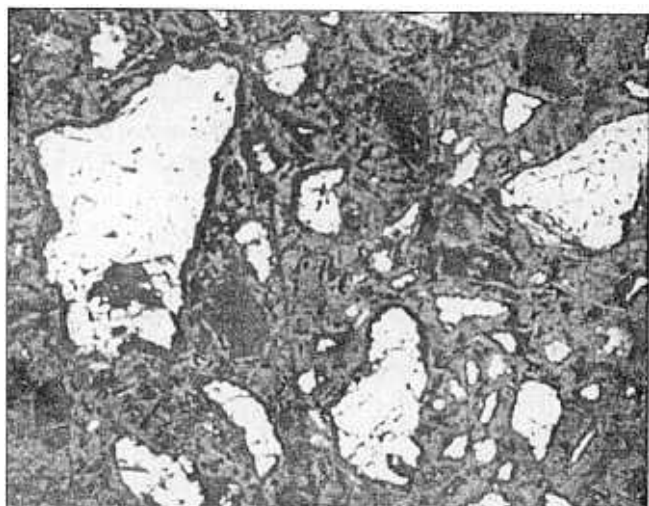
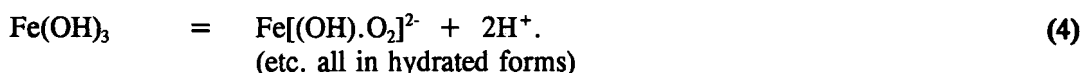
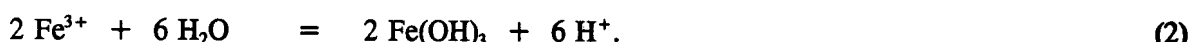
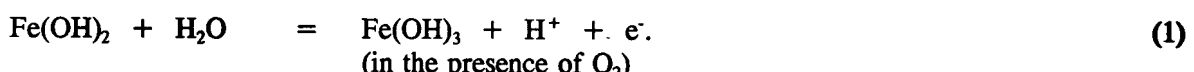
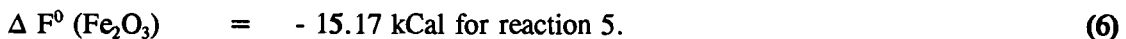
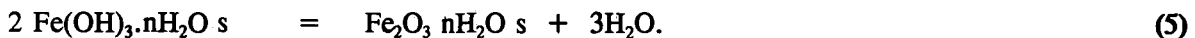


Figure 8. BEI photographs of natural, pyrrhotite hardpan showing FeS grains embedded in goethite matrix.

Although the presence of Fe^{2+} prevents the air oxidation of the tailings in the inner core, the Fe^{2+} in the leachate will eventually add to the acidity owing to hydrolysis reactions as shown below.



The standard free energies of formation (Garrels and Christ, 1965) of the hydrated iron oxides from Fe(OH)_2 and Fe(OH)_3 are fairly negative (equations 5-8). Hence, these hydroxides are unstable and should decompose to hematite (goethite) and magnetite as found in the hardpan.



However, this decomposition will be slow because the activities of the reactants and products (solids) are unity. The hardpan formation is therefore time dependent, but the kinetics can be significantly accelerated by modifying the techniques of surface chemical treatment. The access of oxygen to sulfide tailings for surface oxidation is also kinetically controlled. Both these factors need to be considered in improving the kinetics of hardpan formation.

The Fe^{2+} concentration to be used needs to be optimized so that it does not contribute to the acidity significantly. Alternatively, the ferrous iron used should be completely oxidized and precipitated on the sulfides as oxyhydrates before loading the lysimeters. The latter procedure in particular will increase the kinetics of hardpan formation to a great extent.

Hardening Effect

The hardening was most pronounced in tailings that were preoxidized in the laboratory, treated with Fe^{2+} , and exposed to air with normal humidity (~50%). Except in lysimeter 2 (with a water head), tailings in all lysimeters had hardened from the top and sides to varying degrees, depending on the availability of oxygen in the bed. The most hardened column was 5, where the laboratory-oxidized tailings were intimately mixed with Fe^{2+} solution and exposed to air under atmospheric conditions. Tailings exposed to extra moist conditions (lysimeter 1, 3 and 4) by passing air saturated with water vapors, appeared to be less hardened; the least hardened column was 4 which was not treated or very little treated with ferrous iron. Hardening and self-compaction appeared to proceed simultaneously. As a result, the beds had developed cracks and detached from the walls at several places with water droplets condensing in the intermediate space. Water was condensing even in lysimeter 5 which was exposed to air under atmospheric conditions. Hence the condensed water was most probably originating from a dehydration process during hardening of the tailings.

E-redox, pH and Fe^{2+} - Fe^{3+} Concentration in the Percolant Solutions

The water percolation rates, pH, E-redox and concentration of dissolved Fe^{2+} - Fe^{3+} in the percolating solutions were measured at the beginning of the curing period 1 and at the end of the curing period 2 and the results are shown in graphical form in (figures 3 and 4), respectively. Before taking the end readings, (fig. 4), the trapped air was removed from the lysimeters (except #2) by slowly filling the units from the bottom with tap water having pH 6.5 to 7. The water was then allowed to percolate through the column.

In the case of lysimeter 2 with continuous waterflow, the flow rate, pH and ferrous-ferric concentration in the percolant solution were monitored for the entire period. These results are also shown in figures 3 and 4 for the beginning and the end periods of this work, respectively.

Because of the free space created between the tailing bed and the lysimeter wall, almost all of the water in percolation tests flowed through the column through this space readily in a short period of time (~400 mL in 10

to 15 min). The rest of the water percolated very slowly, most probably through the centre core which was not hardened and remained soft. These two rates are referred to as fast and slow flow rates in fig. 4.

At the starting stage prior to curing period 1 (fig. 3), the pH of the percolant solutions was between 5 and 6 for all columns except that lysimeter 3, with naturally oxidized tailings, had a pH of 4.5. This is because the tailings for this lysimeter were oxidized by exposing to open air in moist condition when much acid must have been produced. This acid was not washed out before lysimeter 3 was loaded and hence accounts for the low pH recorded. The iron content of the percolant solutions in all these runs was also high (0.01 to 0.001M) because the columns were freshly treated with Fe^{2+} solutions.

The pH values of the percolant solutions recorded at the final stage of the work and the redox potentials are given in fig. 4. These pH values range from 5 to 5.5 for lysimeters 1, 3, and 4, while column 5 shows a pH of 5.94 and the pH for column 2 (with a constant water head) continue to be well above 6. The lowest pH recorded was 4.92 for column 3, as before. Except for lysimeter 2, the dissolved iron concentration (almost entirely as Fe^{2+}) was rather high, in the range of 0.01 to 0.005M. As discussed earlier, this high concentration of iron in the leachate is originating from the inner core of the tailings as the adsorbed Fe^{2+} in this region is not oxidized and precipitated as $\text{Fe(OH)}_3\text{-Fe}_2\text{O}_3$ owing to insufficient oxygen supply.

Behavior of Tailings in Lysimeter 2, under 2 in of Water

The pH of the percolant solution from tailings under 2 in of water was initially 5.5 and became clear in about 6 days, the Fe^{2+} concentration being in the m mole range. The pH in later stages was between 5.5 and 6.0, and the Fe^{2+} concentration kept decreasing steadily to μ mole range (fig. 3). In the final stages of work, as shown in fig. 4, the pH was 6.6; E-redox was -0.023 V(SCE), which is highly reducing; and Fe^{2+} concentration was 10^{-8} M with no sign of Fe^{3+} present in the percolant solution. The percolant was practically pure water, once excess of Fe^{2+} (added initially) was removed. Although the bed had compacted well during the curing period, there was no sign of hardening or hardpan formation.

In one experiment, the pyrrhotite column in lysimeter 2, at the final stage of work, was left filled with water without draining it for a week, followed by draining the water and measurement of pH and dissolved iron concentration. In another experiment, the tailings in column 2 were left dry without any water head for a week, and water was then allowed to percolate through. In both these experiments, the pH of the percolant solution was still close to neutral while Fe^{2+} concentration continued to stay low (10^{-8} M). The untreated tailings under the same conditions would produce both acid and Fe^{2+} .

Redox Potentials

Redox potentials of 0.046, 0.120, and 0.186 V(SCE) were measured in solutions percolating from lysimeter 5, 2 and 1, respectively, at the beginning (fig. 3). These potentials, although fairly positive in relation to the standard hydrogen electrode, are still in the cathodic range in regard to charge transfer reactions with pyrite and pyrrhotite (Ahmed, 1990, 1991). As a result, in this potential range, Fe^{2+} can still donate electrons and provide cathodic protection to the sulfide from the atmospheric oxidation.

The redox potentials shown in fig. 4 were measured in the percolant solutions at the final stage, after curing period 2. In general these potentials (fig. 4) are more negative than those at the beginning (fig. 3) and indicate reducing or cathodic conditions available at the FeS-solution interface with respect to $\text{Fe}^{2+}\text{-Fe}^{3+}$ couple. There was experimental evidence to show that the redox potentials inside the bed were more negative than those measured outside, in the presence of air. Under these conditions, oxidation of sulfides by oxygen and Fe^{3+} by electrochemical mechanisms is not possible, although oxygen may still chemically attack pyrrhotite if it is not passivated and protected by iron oxide films.

Stability of Hardened Tailings

The hardened part of the tailings appeared to have good physical stability to withstand water percolation upto a pH of 4.5. In addition to the fully oxidized (type O) forms of the FeS hardpan which are porous and brownish in color, a gray type of unoxidized (type R) FeS hardpan was also encountered in the present work. The type R can be obtained by treating fresh and unoxidized FeS tailings with Fe^{2+} and exposing to air under moist or slightly wet conditions. After a few weeks, a hard and a very dense compact pan is formed which is gray in color and resistant to oxidation in dry or moist air because of the presence of Fe^{2+} in solid state. However, on immersion in water, surface reactions take place, leading to dissolution and precipitation of brown oxyhydrate of iron as a loose precipitate. The hardpans found in nature are usually a mixture of type O and type R hardpans. These hardpans can be completely stabilized by converting the iron oxide surface into less soluble compounds (solubility $< \mu\text{M}$) of iron such as silicates and carbonates, as suggested by phase diagrams (Garrels and Christ 1965).

Summary and Conclusions

1. Pyrrhotite hardpans can be prepared on a small scale by surface chemical treatment of the FeS tailings with Fe^{2+} under controlled conditions of pH, moisture, and oxygen supply. Such hardpans could also be made by cathodic treatment of the FeS tailings followed by exposure to air. The synthetic and natural hardpans were found to have the same structure, consisting of the FeS grains cemented in a ferric oxyhydrate matrix (goethite + lepidocrocite). The hardpan is formed as a result of the oxidation of the adsorbed Fe^{2+} to the ferric state on FeS surfaces and precipitation of the oxyhydrates in the intergranular spaces. The ferric oxyhydrates then seem to consolidate into a hardpan on aging. Natural hardpans of pyrite are rare in occurrence and have slightly different structure at the pyrite-goethite interface.

2. In large scale experiments using lysimeters, formation of hardpans by surface chemical methods was restricted only to the outer layers well exposed to air. The inner core of tailings which was devoid of oxygen, remained soft and retained Fe^{2+} in the unoxidized form. The presence of ferrous iron provides cathodic protection to FeS from air oxidation. During water percolation, however, the excess Fe^{2+} ions drain out and contribute to the acidity of the percolant solution. Hence, the Fe^{2+} concentration to be used, the pH conditions and aeration methods need to be optimized in the hardpan formation.

3. The formation of hardpan is time dependent and is a slow process due to various factors such as low concentration of the dissolved oxygen in water and its slow diffusion to FeS, if immersed in water. Hence, the oxidation rates of FeS are known to be greatly enhanced in moist conditions where the oxygen has to diffuse through only a few molecular layers of water on the surface compared to tailings in wet conditions under several inches of water. The galvanic cells could be formed on FeS surfaces even in moist conditions. Formation of $\text{Fe(OH)}_3\text{-Fe}_2\text{O}_3$ is also kinetically slow (eqns. 5-8), as discussed earlier.

Fast methods of forming FeS hardpans can be developed by improving the reaction kinetics of the processes involved. In addition, the $\text{FeS-Fe}_2\text{O}_3\text{.nH}_2\text{O}$ hardpans can be further stabilized by converting the iron oxide surfaces into less soluble compounds of iron such as silicates, by surface chemical methods. This would greatly reduce the equilibrium concentration of the dissolved iron and hence the acidity in the percolant solutions.

4. Whereas the oxidation of pyrrhotite by oxygen is predominantly chemical, the oxidation of pyrite is mainly electrocatalytic in nature. Hence, formation of iron oxide films on pyrite is difficult without changing the surface composition significantly. The present, surface chemical methods therefore were not applicable to pyrite for hardpan formation.

5. The presence of an iron oxide layer on the FeS surfaces would substantially reduce the cross section of the sulfide exposed to oxygen attack. The use of Fe^{2+} would further reduce the oxygen flux by reacting with it and eventually forming the ferric oxyhydrate in the inter granular space.

6. The oxidative decomposition of the FeS and of the acid generation can be completely prevented by maintaining about 2 in of water head on the top of the tailings. This effect is not merely due to the lowering of the oxygen flux at the surface and its slow diffusion kinetics as discussed above, but also due to the formation of Fe²⁺ ions formed from FeS oxidation. The Fe²⁺ provides cathodic conditions to the surface in addition to reacting with oxygen directly as discussed above. Hence treating the tailings with a dilute solution of Fe²⁺ further helps in the protection of FeS from oxidation. However, the concentration of Fe²⁺ to be used needs to be optimized so that it does not contribute to the acidity of the percolant solution significantly.

In field conditions, the existing beds could be treated with the minimum amount of Fe²⁺ to prevent air oxidation and the bed could then be topped with a hardpan formed as above. The iron oxide in the hardpan need to be further stabilized by converting the surface into less soluble compounds of iron so as to completely prevent the dissolution of iron. For new tailings, the entire bed could be converted into a hardpan by applying a fast method of hardpan formation by treating with Fe³⁺ in low concentration, followed by hydrolysis. Certain optimization studies need to be conducted in this respect before a large scale method could be developed.

Acknowledgement

The help from M.T. Skaff in the initial treatment of tailings and setting up of the lysimeters was significant and is gratefully acknowledged.

Literature Cited

- Ahmed, S.M. and Giziewicz, E., 1992. Electrochemical studies of iron sulfides in relation to the atmospheric oxidation and prevention of acid drainage, Part II. Proc. Third Intern. Symp., Electrochemistry in Mineral and Metal Processing, May 1992, St. Louis, ed. P. Richardson and Ron Woods, p. 403-415.
- Ahmed, S.M., 1991. Electrochemical and surface chemical methods for the prevention of the atmospheric oxidation of sulfide tailings. Proc. Second Intern. Conf. on the Abatement of Acid Drainage, Montreal, Sept. 1991, Pub. MEND, Vol. 2, 305-320.
- Ahmed, S.M., 1990. Electrochemical studies of semiconducting pyrite in relation to its atmospheric oxidation and chemical leaching. Electrochem. Soc. 178th Meeting, Seattle, WA, Oct. 14-19. Abstract No. 725.
- Garrels, M.R. and Christ, L.C., 1965. Solutions, Minerals, and Equilibria. Harper and Row, New York, p. 182.

**INTERNATIONAL PERSPECTIVE ON THE ROLE
OF ACID GENERATION IN SELECTING DECOMMISSIONING TECHNIQUES
FOR URANIUM MINING SITES IN EASTERN GERMANY¹**

D.G. Feasby², D.B. Chambers³, J.M. Scharer³,
C.M. Pettit³, R.G. Dakers⁴ and M.H. Goldsworthy⁵

Abstract: The control of acidic drainage from uranium mine wastes in Germany is a significant component of mine site rehabilitation that began in 1992. Uranium was mined on a very large scale in the States of Thüringen and Sachsen from 1946 to 1991. Sulfide oxidation creates acidic drainage from waste rock piles at several mine sites and may occur in the future at two tailings impoundments. The extent of the problem of acidic drainage and methods to control acid production are reviewed from an international perspective. A central component of the rehabilitation plans in Germany is a proposal to fill a large open pit with acid-producing waste rock, allowing it to flood, and treating the overflow. This plan is assessed using a regional geological model in a probabilistic framework. This modeling has proven to be a useful tool in assessing management alternatives.

Background

Starting in 1946 and ending in 1991, uranium was mined on a large scale in the States of Thüringen and Sachsen in southeastern Germany. The scale of uranium mining in this area made it one of the world's largest uranium producers. The mining and uranium recovery was undertaken in the former East Germany by U.S.S.R.-German Democratic Republic company, Wismut. In addition to the recent mining for uranium, mining of these areas had been carried out since the Middle Ages for iron, silver, and other metals including bismuth (Wismut 1992). Following the reunification of Germany and the closure of the mines, major work and environmental assessment have been performed to decommission both the Wismut and historic sites. The authors have participated in assisting the Bundes Ministerium für Umwelt Naturschutz und Reaktorsicherheit (BMU) in their ongoing review of the Wismut decommissioning programs.

Over 1,600 sites in the mining region have been identified as having greater than background levels of radioactivity. Most of these sites have been linked to previous mining activity. The major mine waste sites of interest are those that resulted from the uranium mining, where approximately 200 million mt of mine tailings and 500 million mt of mine waste rock have been deposited on surface. The major uranium mining and mineral processing sites were those of the Wismut company; their locations are shown in figure 1.

An inventory of the major wastes remaining on surface is summarized in table 1. Acid generation resulting from the oxidation of sulfide minerals has been identified as a major concern in the mines and waste rock heaps on surface and underground at Ronneburg and is a potential concern at Königstein. In addition, there is a potential problem in two of the tailings basins at the Seelingstädt site, where ores were processed by acid and alkaline leaching to recover uranium.

¹For presentation at the Third International Conference on Abatement of Acidic Drainage. Pittsburgh, Pennsylvania, U.S.A., 25-29 April 1994

² Mineral Sciences Laboratories, CANMET, Ottawa, Canada

³ SENES Consultants Limited, Toronto, Canada

⁴ Consultant, Ottawa, Canada

⁵ Golder Associates, Celle, Germany

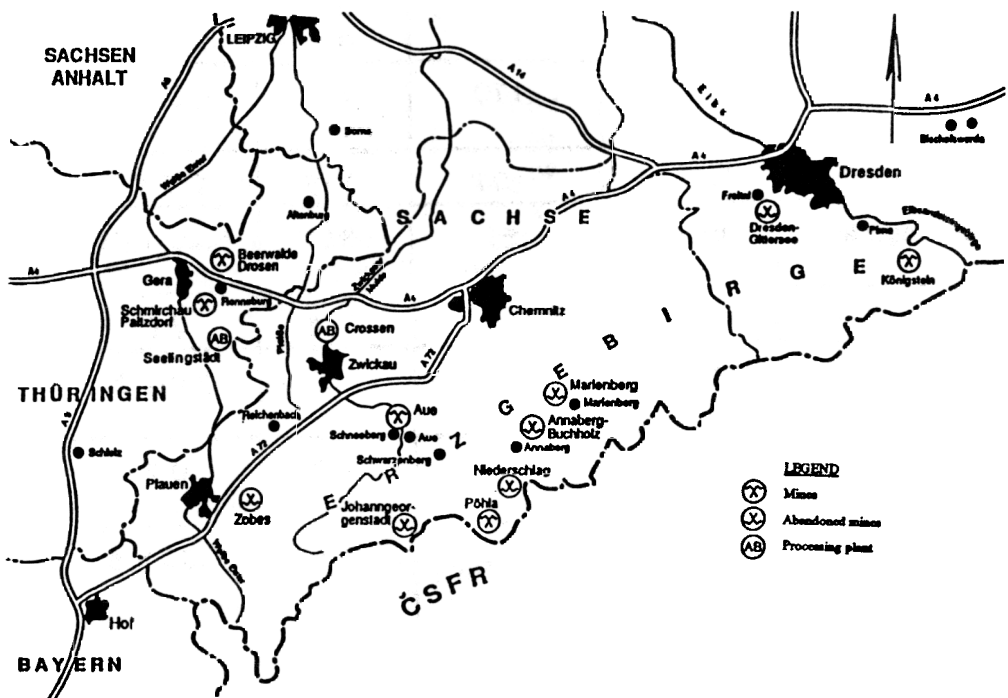


Figure 1. Location of Wismut mining works

ACKNOWLEDGEMENT

The authors gratefully acknowledge the permission of Wismut GmbH to publish this paper. The patient assistance of Dr. Daenecke and his staff in providing the needed information is very much appreciated.

TABLE 1 SUMMARY CHARACTERISTICS OF URANIUM MINE WASTES

Location	Waste type	Volume million m³	Surface area, ha	Radium Bq/g	Pyrite, %
Ronneburg	Waste rock	170	409	0.3-1.5	3.3-4.8
Seelingstädt	Tailings	104	335	6.7-12	Variable*
Seelingstädt	Waste rock	59	519	0.25-1.65	NA
Crossen	Tailings	45	213	6.0	NA
Crossen	Waste rock	2	22	2.0-2.3	NA
Aue-Schlema	Waste rock	47	343	0.2	NA
Königstein	Waste rock, treatment sludges	3.3	25	0.34-5.6	1-2

NA Not available

Bq/g Becquerel/gram

* Acid leach tailings 0.8% to 5%, alkaline <1%,

Because of the very large quantities of these sulfide-bearing wastes, minimizing acid generation is a critical element in the decommissioning of the sites. The concerns are not only the production of acid waters and their effect on the environment per se, but also the leaching of radioactive species and heavy metals into ground and surface water and their subsequent dispersal in the environment. In addition, if significant acid generation continues to occur, there will be a need to collect and treat water for possibly hundreds of years. Ongoing water treatment also requires ongoing management of water treatment sludges, which contain radioactive and other heavy metals.

This paper describes the acid generation sources and magnitude of the problem and implications for decommissioning these former uranium mining areas.

The Impact Of Acid Generation in Uranium Mine Wastes

Experience in Canada and elsewhere has led to the conclusion that sulfuric acid generation is one of the major concerns associated with the decommissioning of sulfide-containing tailings and waste rock areas. Acid-leached uranium tailings are often significant acid producers even though the sulfide mineral content in the ore may originally have been very low. Strong acid generation can occur because most or all of any natural mineral alkalinity has been removed in the uranium extraction process by a hot sulfuric acid leach.

The chemistry of acid generation has been reviewed in detail (Nordstrum 1982) and can be summarized by the following reactions:



Although these reactions can occur in a biologically sterile environment, chemolithotrophic bacteria, particularly Thiobacillus ferrooxidans, can accelerate the iron oxidation rate. Ferric iron in acidic solution can also oxidize metal sulfides (MS) according to



Low pH (<4.0) seepage waters are often associated with mine wastes where sulfide oxidation is occurring, but frequently alkaline minerals such as calcite or dolomite present in the wastes can neutralize the acidity produced and near neutral conditions (pH ~ 7) can result *until the alkaline minerals are consumed or rendered unreactive by surface coatings*. Acidic drainage from mine wastes will solubilize many metals including aluminum, copper, zinc, nickel, manganese, and lead. For uranium-rich deposits, uranium and thorium are also dissolved. Blair et al. (1980) have identified metal contaminants mobilized by acid production as the most important concern in the management of pyritic uranium tailings. Also, acidic drainage has been identified at uranium mine waste rock sites in Australia by Ryan and Joyce (1991). Waste rock piles are very porous to water and oxygen, essential ingredients for sulfide oxidation; because the piles are usually constructed on porous foundations, this "acid rock drainage" has been very difficult to prevent and control at sites around the world.

Acidic drainage is a significant environmental concern at the former uranium mining area in the States of Sachsen and Thüringen, Germany. High levels of acidity and dissolved metals are found in drainages at several locations. At one location, Ronneburg, autogenous combustion caused by rapid oxidation of sulfide sulfur and carbon (graphitic carbon) had caused additional problems in mining and waste disposal. Significant quantities of sulfide minerals (notably pyrite) are also present in the waste rock at Crossen, Aue, and Königstein. Although most drainages sampled to date indicate neutral drainage, elevated levels of dissolved calcium and magnesium sulfates indicate that the possibility of future acid generation in these wastes cannot be excluded.

Site Considerations

Ronneburg-Drosen

The Ronneburg-Drosen mines are in east Thüringen, Wismut's most important uranium mining area. In total, these mines produced over 170 million m³ of waste rock, all of which is potentially acid generating. At present, over 100 million m³ of waste rock are stored on surface (in 14 waste piles). One pile was subjected to in situ uranium leaching using mine water supplemented with sulfuric acid. The remainder had been placed in a large open pit. Like most of the waste piles in southeastern Germany, the waste piles are located close to villages and individual homes (within several hundred meters). In addition to the understandable concerns about environmental radioactivity, particularly radon emissions, there are concerns about contamination of surface water and ground water and physical access to the materials. A cross section of the most environmentally significant part of the mining area at Ronneburg is shown in figure 2. Mining ceased at Ronneburg in December 1991, and the lower levels of the mine are now being allowed to flood.

Current plans (Wismut 1992) are to fill the open pit with as much waste rock as possible. The most severe acid producers will be placed on the pit bottom, but about 30 million m³ will remain above the water table. The final contouring and cover applied to these materials will be important factors in determining long-term acid production. Excess alkalinity, for example, lime and/or limestone, is being considered to help control acid generation, and studies were recently completed to determine the effect of submerging most of the waste rock under the water table in the open pit.

Until the mine workings are flooded, acid will continue to be produced from sulfide minerals in open spaces and fractured zones underground. In addition, in the long term after the mines are flooded, acid will continue to be produced in the fractured ground above the water table.

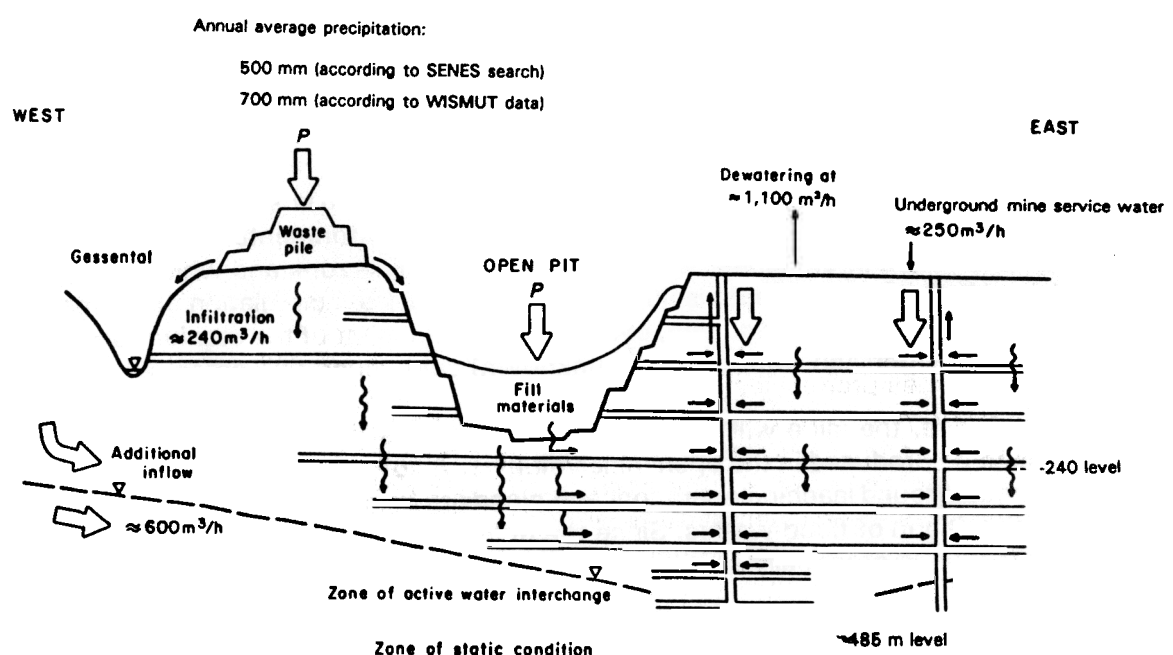


Figure 2. Wismut Decommissioning
Ronneburg Site Existing Hydrological Situation Typical Conceptual E-W Section

Seelingstädt

Seelingstädt was a central ore processing facility for the Wismut mines. Uranium was extracted from the ore in parallel circuits, one with alkaline sodium carbonate, and the other with sulfuric acid. The sulfuric acid circuit was used to leach uranium from high sulfide ores and pyrite concentrates. Tailings from the acid circuit are potential acid producers if dewatered and exposed to oxygen. The tailings from the alkaline circuit represent no acid generation potential because the pyrite was converted to soluble sulfate by the following reaction:



Available data (Wismut 1992) indicate potential for acid generation in two large tailings basins at this site. At present, the basins are water saturated, and much of the formerly exposed tailings surface is covered with soil. The conceptual plan (Wismut 1992) is to dewater the tailings pond and to cover the balance of the dewatered tailings with a soil cover. Dewatering has the potential to result in increased oxidation and acidification of sulfide minerals, even though the pore fluids are currently alkaline from the mixing in of alkaline chemicals used in the milling process.

With respect to tailings and acid generation, the situation at Seelingstädt is unique; acid leached tailings are covered with alkaline water (pH 7.4 to 9.9) with high levels of dissolved sulphates (10 G/L). However, any residual mineral alkalinity has been removed in the acid leaching process, and if the tailings are dewatered as planned, infiltration of rainwater could flush out these buffering salts and permit acid generation to start. Based on the appearance of ferric iron salt coloration on exposed tailings beaches, this acidic generation potential appeared to be confirmed.

There is considerable international experience in predicting the rate of acid generation in pyritic mine tailings, and estimates of the rate of acid production by sulfide-bearing uranium tailings have been given by Halbert et al. (1983) and Scharer et al. (1991). Acid-base accounting on field samples (Wismut 1992) has shown that the acid-leached tailings are potentially acid generating; precise predictions cannot be made until the decommissioning scenario (eg., dewatering and covering) is established.

Königstein

The Königstein site in Sachsen has extensive underground workings, which were initially developed by conventional mining, and more recently by underground in situ leaching with sulfuric acid addition to leach solutions recirculated from surface. The key environmental concern at this site is the potential for contamination of an aquifer which overlies the mining zone and which is used for drinking water. About 1 million m³ of acid leach solution has been lost from circulation and is presently in the pore space in the fractured rock. In addition, pyrite is present in most of the uranium-bearing zones, and these strata represent significant (but currently unknown) acid generation potential.

In the near future, the mine will be flooded, and acid production will cease, but until such time acid will continue to be produced in the open mine volumes. Also there will remain considerable residual acidity from the underground leaching operation, and plans are being developed to neutralize this acidity on surface by recirculation of flood waters. Since the underground workings cover 5 km², the effect of the natural acidification is potentially significant.

Also at Königstein, there exists a 3.2 million m³ surface waste pile, which is composed of 2.0 million m³ of heap leach waste rock and other wastes, principally uranium-barren waste rock and water treatment sludges. The main concern with respect to acid generation is the heap leach pile. Although it has been depleted in sulfide sulfur content by bacteria-catalyzed oxidation, oxidation of the estimated remaining 1% to 2% pyrite content could accelerate in the near future. Currently, the waste pile produces an acidic effluent, as shown in table 2

TABLE 2 ACIDIC DRAINAGE FROM KÖNIGSTEIN WASTE ROCK

Volume	3 to 10 m ³ /h
pH	2 to 4
U	30 mg/L
Ra	0.5 Bq/L
Fe (total)	200 mg/L
SO ₄	3000 mg/L

Technical Considerations for the Prevention and Control of Acid Production

Various interdependent geochemical, physical, and biological factors control the rate and quantity of sulfide oxidation in the waste rock and tailings. These factors include temperature, bacteria activity, oxygen profile, pore water composition, effective grain size of sulfide minerals, and acid neutralization potential.

As an example of currently available predictive techniques, the authors have recently completed an extensive review of the environmental impact of depositing acid-producing waste rock into the bottom of the open pit at Ronneburg. To develop a reference point for environmental assessment, a waste rock pile that had formerly been a heap leach for uranium recovery was selected for evaluation. A computer model (ACIDROCK) was used to simulate the placement and leaching history of the waste rock pile (SENES 1993a). The model was used to predict the long-term seepage quality for various management options (e.g., covered with an engineered soil cover, and uncovered). The results of modeling the 27-ha pile showed that -

- Acidity will be produced for more than 100 years, with or without cover;
- A state-of-the art earth cover will reduce acid production and water treatment requirements by an order of magnitude;
- Continuous care and maintenance of the site would be required.

A much more complex predictive modeling evaluation was completed on the option of placing the same waste rock pile into the bottom of the pit. Geochemical measures, such as the addition of lime to neutralize acidity contained in the waste rock, were considered as part of the evaluation. The first stage of the modeling was the development and application of a hydrological model that simulated the flooding process, the establishment of steady-state flows with all of the mine cavities filled with water, and the contaminated ground water emerging at a nearby stream valley (Brenk Systemplanung 1993). A filled pit in the flooded condition is shown in figure 3.

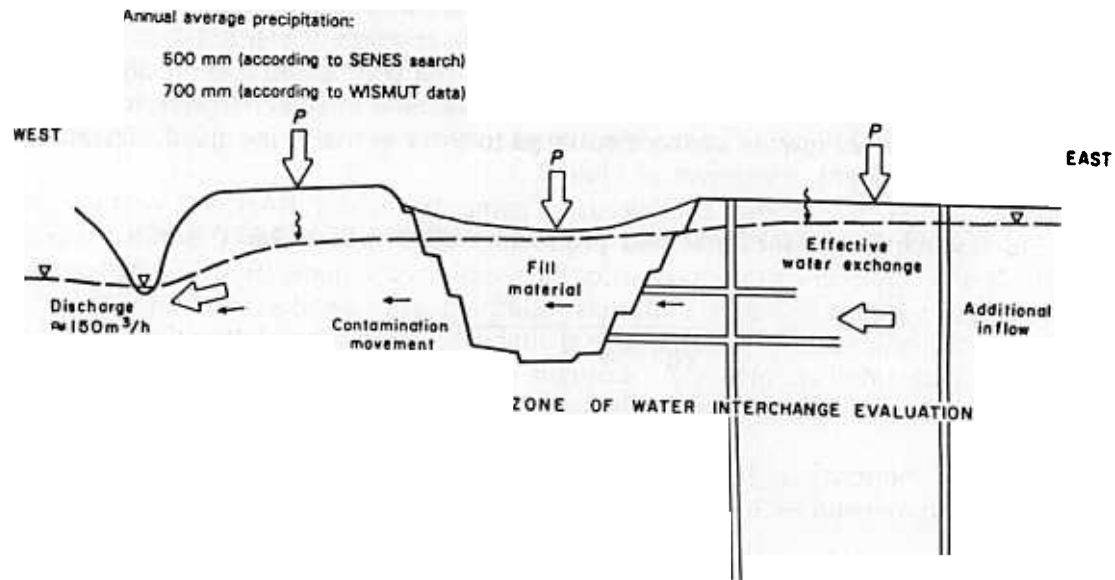


**Figure 3. Wismut Decommissioning
Ronneburg Site Future Hydrological Situation Typical Conceptual E-W Section**

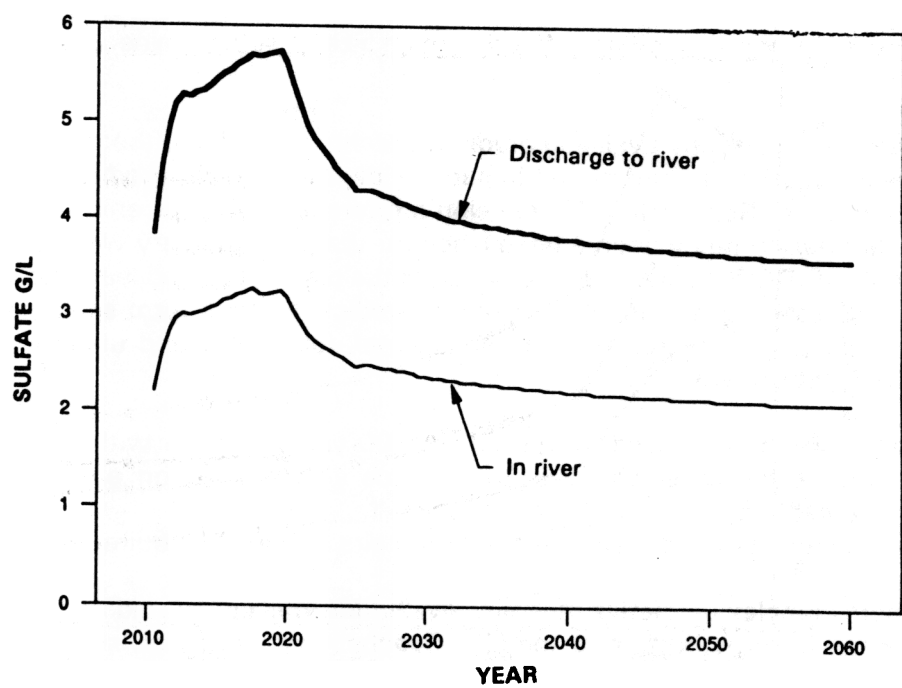


Figure 4. Predicted Sulfate

A computer model (ROCKSTAR) was used to simulate the geochemical processes occurring in the flooded pit materials and the associated underground mining areas (SENES 1993b). The model was used deterministically to predict the water quality within the pit fill and mining areas, as well as the water quality of the surface water body (river) that would receive the discharge from the mining region. Figure 4 shows the predicted quality of the discharge to the river, and the quality in the river.

Probabilistic modeling was also employed. A computer model (RANSIM) was used to randomly select many input values from the specified probability distributions for the key model parameters (SENES 1989). These values are substituted into the geochemical model (ROCKSTAR) to obtain a single value for each output variable. This procedure is repetitive, with each selection being referred to as a trial. Using the probabilistic approach, subjective probability distributions rather than single numbers will be obtained for the calculated variables. An example of the predicted water quality of the discharge to the river for 50 trials of the probabilistic model is shown in figure 5.

The predictive modeling assessment of placing the heap leach waste rock into the pit at Ronneburg can be summarized as follows:

- Nearby mine openings and underground broken rock zones control water flow patterns. (The underground mine excavations included over 1,800 km of tunnels).
- The contained acidity and stored oxidation products of the waste rock had a small impact on the emerging water quality.
- The addition of lime to the waste rock reduced the predicted impact of the waste rock to insignificant levels (reduced sulphate and metal mobility).

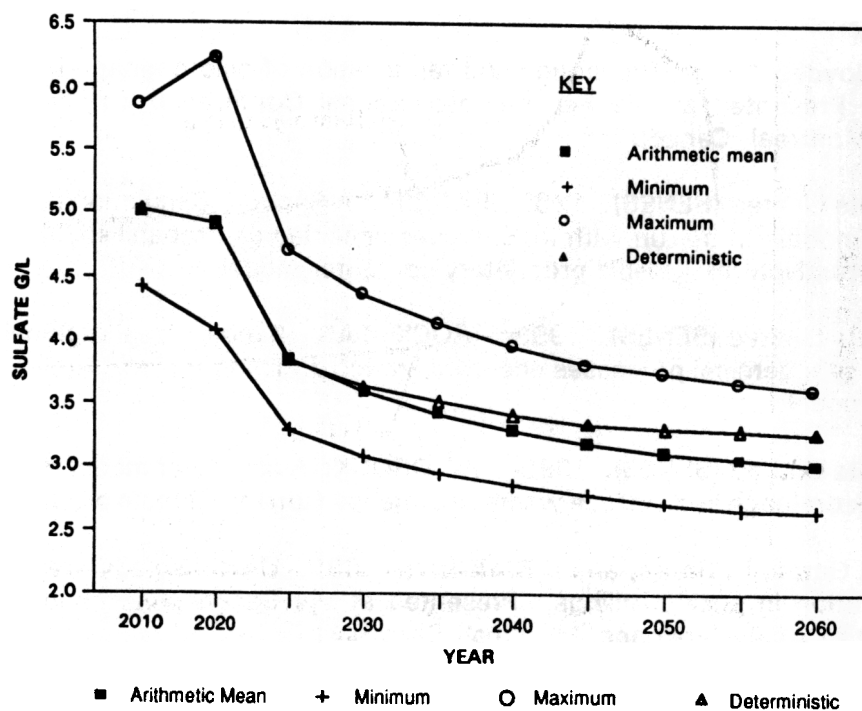


Figure 5. Predicted Water Quality for Discharge to River
Probabilistic Approach - 50 Trials

Summary

Control and treatment of acid rock drainage is a major focus of the decommissioning strategies being developed for the uranium mine sites in south eastern Germany.

Sophisticated mathematical models are being applied in the evaluation of mine decommissioning technology, which includes prevention and control of acidic drainage from waste rock and tailings. A major focus of the control measures for waste rock is depositing the rock into an open pit and then allowing the pit to flood with mine waters. Worldwide, the evaluation of options for dealing with acid-producing waste rock and tailings has led to the selection of the use of water covers and underwater disposal as the best technology.

References

- Blair, R.D., J.A. Cherry, C.P. Lin, and A.J. Vivyurka. 1980. Groundwater monitoring and contaminant occurrence at an abandoned tailings area, Elliot Lake, Ontario. Presented at the First International Conference on Uranium Mine Waste Disposal, Vancouver, Canada.
- Brenk Systemplanung. 1993. A three dimensional finite element model for simulating groundwater flows in a mining region.
- Halbert, B.E., J.M. Scharer, R.A. Knapp, and D.M. Gorber. 1983. Determination of acid generation rates in pyritic mine tailings. Presented at the Annual Conference of the Water Pollution Control Federation, Atlanta, GA.
- Nordstrum, D.K. 1982. Aqueous pyrite oxidation and the consequent formation of secondary iron minerals in acid sulphate weathering. *Soil Sci, Soc, America*, p. 37-55
- Ryan, P. and C. Joyce. 1991. Prevention and remediation of acid drainage from mine waste rock in Australia. Presented at the Second International Conference on the Abatement of Acidic Drainage, Montreal, Canada.
- SENES Consultants Limited (SENES). 1989. RANSIM: A Random Simulation computer model to allow FORTRAN models to be run with input values specified as probabilistic distributions rather than as constants. Non marketable proprietary computer model.
- SENES Consultants Limited (SENES). 1993a. ROCKSTAR: A multi-nodal regional computer model for simulating geochemical processes occurring within a mining region. Non marketable proprietary computer model.
- SENES Consultants Limited (SENES). 1993b. ACIDROCK: A computer model for simulating production of acid rock drainage in a surface waste rock heap. Non marketable proprietary computer model.
- Scharer, J.M., V. Garga, R. Smith, and B.E. Halbert. 1991. Use of steady-state models for assessing acid generation in pyritic tailings. Presented at the Second International Conference on the Abatement of Acidic Drainage, Montreal, Canada.
- Wismut. 1992. Umweltbewertung des gesamtkomplexes tagebau-flutung-halden (Environmental evaluation of the total complex - open pit). Wimsut 30.9).

EVALUATION OF ACID GENERATING ROCK AND ACID CONSUMING ROCK MIXING TO PREVENT ACID ROCK DRAINAGE¹

Stephen J. Day²

Abstract: Mixing acid generating and acid consuming rocks is an attractive and potentially low cost alternative for in situ prevention of acid generation in waste rock piles at some mine sites. In addition to the practicalities of day-to-day management of mixed waste rockpiles, the success of the mixing will probably depend on the proportion of acid-consuming material, the availability of the acid consuming minerals, and the intimacy of mixing. A 5-yr column study for the Cinola Gold project, an epithermal gold deposit located in a cool, moist maritime area of northwestern British Columbia, Canada, was initiated in 1988 to evaluate limestone requirements to prevent acid and metal release from waste rock stockpiles. Limestone content in five columns varied from zero (control, net neutralization potential = -58 kg/mt CaCO₃) to 6.6% (NNP = 7 kg/mt CaCO₃). Four of the columns generated acid. The column containing the highest concentration of limestone did not release acid, although residues in the upper part of the column were acidic and sulfate concentrations in leachate were gradually increasing. It was concluded that (1) the actual quantity of limestone required to prevent acid drainage in perpetuity would probably be at least twice that determined by conventional acid-base accounting, (2) limestone availability was not reduced by ferric hydroxide coatings, (3) the time required for marginally acid generating rock to release acidity increased exponentially as the quantity of limestone increased, and (4) the time required for zinc release to begin increasing was linearly proportional to the neutralization potential. Limestone addition was therefore highly effective in delaying acid release but was less effective in delaying zinc release.

Additional Key Words: acid rock drainage, waste rock, alkaline addition.

Introduction

Many potentially economic mineral deposits contain high concentrations of iron sulfides and therefore waste rock, mine workings and tailings associated with such deposits are prone to acid generation. However, a significant number of deposits also have associated acid consuming minerals in the mineralization or nearby host and country rocks. In some situations, the possibility of mixing acid generating and acid consuming rocks is an attractive and potentially low cost alternative for in situ prevention of acid generation. When correctly engineered, mixing (or blending) may yield a long term waste management solution without the long term liability and maintenance of artificial structures such as dry covers, artificially flooded impoundments, or water treatment plants.

This paper presents results for a 5-yr column leaching study conducted on marginally acid-generating materials. The study was initiated by City Resources (Canada) Inc. to evaluate the inhibition of acid generation by adding limestone to stockpiles of potentially acid-generating rock at the proposed Cinola Gold Project in northwestern British Columbia (BC). The limestone is not naturally available at the site but is found on an island off BC.

General Background

A number of uncertainties remain regarding design of mixed rock waste piles. Although some of these uncertainties relate to the practicalities of day-to-day management of such piles under operating conditions, a more

¹ Paper presented at the International Land Reclamation and Mine Drainage Conference and the Third International Conference on the Abatement of Acidic Drainage, Pittsburgh, PA, April 24-29, 1994.

² Stephen J. Day, Senior Geochemist, Norecol, Dames & Moore, Inc. 500-1212 West Broadway, Vancouver, British Columbia, Canada, V6H 3V1.

fundamental issue relates to the amount of neutralizing material required to effectively consume acid produced by oxidation of iron sulfides.

The commonly used acid-base accounting procedure represented one of the first attempts to determine an acid producing-consuming balance in heterogeneous materials (Sobek et al. 1978). The theory was based on the assumption that neutralizing minerals (represented by calcium carbonate) are consumed completely to release carbon dioxide (gaseous or dissolved). In reality, the initial phases of acid generation occur under approximately pH-neutral conditions and carbonates neutralize acid incompletely, forming the bicarbonate ion (HCO_3^-). In natural rock mixtures, other considerations arise, such as the heterogeneous distribution of sulfide and carbonate minerals, the slow dissolution of carbonate minerals in the absence of acid, and the coating of carbonate grains by precipitated hydroxides. In recognition of these uncertainties, regulators in some jurisdictions (for example, California and British Columbia) require that blended rock mixtures at metal mines contain at least three times as much neutralizing material as acid generating material (both expressed in equivalent concentration units of calcium carbonate). Some support for these requirements can be found in the data from coal mines in the eastern United States which indicate that the ratio of neutralization potential to potential acidity in waste rock should be at least 2.4 to ensure acid is not released (Cravotta et al., 1990).

One of the difficulties in determining acceptable mixing ratios is that results from laboratory and field tests tend to be inconclusive. The success of a mixing approach is shown by the lack of acid generation. The problem is that most tests are not continued to a definitive end point which indicates that acid will not be produced. Ferguson and Morin (1991) showed that the time for acid to be produced increases exponentially as the ratio of neutralization potential (NP) to maximum potential acidity approaches 1. Any experiment designed to address marginal acid generating conditions must operate for an extended period (often several years) to demonstrate conclusively that acid will not be produced.

Cinola Project Background

The Cinola Gold Deposit is located on the Queen Charlotte Islands off the north BC coast. The deposit is classified as epithermal Carlin-type by Champigny and Sinclair (1982) owing to the small ($<0.5 \mu\text{m}$) particle size of gold, age of about 14 million years, presence of argillic alteration, association with faults and felsic intrusions, and porosity of the host rock. Disseminated, fine-grained ($<25 \mu\text{m}$) sulfide minerals (primarily pyrite, with lesser marcasite) occur throughout the mineralization and host rocks, generally in concentrations of a few percent. In contrast, calcite occurs sporadically, and in one important unit, the Skonun Sediments, is almost completely absent. Acid-base accounting indicated that the Skonun Sediments are potentially acid generating. Laboratory and field kinetic tests confirmed that acid would be produced.

The region hosting the deposit experiences seasonal weather patterns typical of coastal western Canada, that is, most precipitation occurs as rain during October to March. Annual precipitation ranges from 1,700 to 2,200 mm. Average monthly temperatures are never less than 0°C . As a result of the high precipitation rate, the potential for mobilization of acid weathering products from waste rock dumps composed of Skonun Sediments is high. Waste rock management was therefore planned to address perpetual prevention of acid generation. It was proposed that the potentially acid generating Skonun Sediments be stockpiled during operation and then backfilled and submerged in the open pit during mine decommissioning. To prevent extensive oxidation and the release of acid rock drainage from the stockpiles prior to submergence, it was proposed that limestone be added to the stockpiles in a controlled fashion. A column leach study was designed to evaluate such factors as limestone requirement, availability of limestone for reaction, and the effect of intimate mixing and layering of acid consuming and acid generating rock.

Experiment Design

Five columns were designed:

- | | |
|----------|---|
| Column 1 | Waste rock only (control test). |
| Column 2 | Approximately 6.6% limestone intimately mixed with waste rock (theoretically sufficient to neutralize maximum potential acidity). |
| Column 3 | Approximately 3.2% limestone mixed with waste rock capped with 1 cm of column 2 mixture (50% of maximum potential acidity). The cap was intended to investigate one dump design option. |
| Column 4 | Approximately 0.84% limestone mixed with waste rock capped with 1 cm of column 2 mixture (acid neutralized for 10 weeks at a rate predicted from humidity cells). |
| Column 5 | Approximately 1.2% limestone as five 1-cm thick layers of column 2 material alternating with four 10-cm layers of column 4 material to evaluate the effects of layering. |

Materials and Methods

Test Materials

Waste rock for the columns was derived from composited reverse circulation drill cuttings from various subgroups of the Skonun Sediments. The composites were designed to approximate the expected composition of waste rock piles. Limestone for the experiments was obtained from Texada Island, the proposed source of limestone if the deposit were developed. The limestone was dried and crushed to a diameter of 0.6 mm or smaller. Limestone and waste rock were mixed on plastic sheets before placement in the columns.

Test Material Characteristics

The waste rock contained approximately 2.1% total sulfur and had a neutralization potential of 8 kg/mt CaCO₃. Net neutralization potential (NNP) was approximately -58 kg/mt CaCO₃. The limestone contained some sulfur (0.22%), and based on the neutralization potential of 932 kg/mt CaCO₃, had a high purity. The dominant carbonate mineral in the limestone was calcite. Dolomite was expected to be a minor component. The surface area of particles was estimated using size fraction analysis and assuming that particles were perfectly spherical. Waste rock and limestone had surface areas of 5.4 and 30.9 m²/kg, respectively. These values are gross approximations but show that the reactive surface area of the limestone was about five times that of the waste rock. The limestone was deliberately crushed finer than the waste rock to yield a greater reactive surface area.

Acid-base accounts (ABA) for the four columns containing limestone (2 through 5) were determined using mass-weighting. Values for each parameter were determined using the formula

$$P_{\text{weighted}} = (P_{\text{lst}} \cdot M_{\text{lst}} + P_{\text{rock}} \cdot M_{\text{rock}}) / (M_{\text{lst}} + M_{\text{rock}}) \quad (1)$$

where P is the parameter (e.g., neutralization potential, NP; maximum potential acidity, MPA), and M_{lst} and M_{rock} are the masses of limestone and waste rock in the column. Values for each column are summarized in table 1. Neutralization potential ratio (NPR) was determined as equal to NP_{weighted}/MPA_{weighted}. Since the quantity of limestone was relatively small, the MPA of the columns varied over a small range (62 to 65 kg/mt CaCO₃). Only column 2 was considered potentially acid consuming from conventional interpretation of ABA. The remaining columns had NNP<0 and NPR<1, implying a potential for net acid generation.

Test Procedures

Test materials were placed in 15-cm diameter plastic columns to a thickness of 0.5 m. Column tops were covered with a plastic plate to minimize evaporation. Holes in the plate allowed humidified air and de-ionized water (at a rate of 0.4 to 0.5 mL/min) to be continuously introduced into the column. The top plate was rotated daily so

Table 1. Acid-Base Accounting - Test Materials and Residues.

Position in column	S, %	Sulfate, S, %	Sulfide, S, %	MPA kg/mt, CaCO ₃	NP	NNP	NPR	Paste pH
Column 1, Control								
Pre-test Bulk.....	2.10	NA	NA	66	8	-58	.12	6.90
Residue Top, bulk.....	.53	.09	.44	17	-2	-19	.00	3.30
Residue Middle, bulk.....	.55	.10	.45	17	-2	-19	.00	3.62
Column 2, 6.6% Limestone								
Pre-test Bulk.....	1.98	NA	NA	62	69	7	1.11	NA
Residue Oxidized, bulk.....	1.12	.05	1.07	35	3	-33	.07	5.30
Residue Non-oxidized, bulk..	1.72	<0.01	1.71	54	57	2	1.05	7.80
Column 3, 3.2% Limestone								
Pre-test Bulk.....	2.05	NA	NA	65	38	-27	.58	NA
Post-test Top, bulk.....	.85	.05	.80	27	0	-26	.01	4.76
Post-test Middle, bulk.....	.77	.11	.66	24	-2	-26	.00	4.05
Column 4, 0.84% Limestone								
Pre-test Bulk.....	2.08	NA	NA	66	16	-50	.24	NA
Post-test Bulk.....	.65	.11	.59	20	-2	-22	.00	4.06
Column 5, 1.2% Limestone in layers								
Pre-test Bulk.....	2.08	NA	NA	66	19	-46	.29	NA
Post-test Bulk.....	.68	.12	.56	21	-2	-23	.00	4.25

NA - Not analyzed.

Pretest results were calculated from mass-weighted averages of limestone and waste rock components

that the introduced water contacted different surface locations. In addition to the direct weekly measurement of conductivity and pH, leachates in the collection vessel were analyzed for sulfate (by a gravimetric method), alkalinity/acidity (by titration with sulphuric acid and sodium hydroxide, respectively), and dissolved (<0.45 µm) metals, which included iron, copper, zinc, arsenic, lead, and the major alkali and alkali earth metals. Metal concentrations were determined by several methods including atomic absorption, flameless atomic absorption and inductively coupled argon plasma (mass spectroscopy). After completion of the tests, the columns were dismantled and examined. Samples of the residues were collected for chemical analysis (acid-base accounting, carbonate and sulphur species) and preparation of polished thin sections for identification of secondary minerals.

Results

Leachate Chemistry

Leachate from all four columns containing some limestone was initially pH neutral (fig. 1). Column 1 (control) generated leachate with pH 3 for about 11 weeks. The pH then dropped to near 2. The pH of leachate from this column then steadily increased to greater than 3. Column 4 (low limestone concentration) and column 5 (layered limestone) both generated acidic leachate at week 33. For both columns, pH dropped to between 2 and 3 very rapidly, without intermediate plateaus. Column 3 (intermediate limestone concentration) generated acidic leachate after about 4 yr of operation. The transition to low pH conditions was not quite as rapid as for columns 4 and 5. The column containing the highest concentration of limestone (column 2) generated pH-neutral water throughout the 5-yr experiment.

Sulfate concentrations in the leachate from each of columns 1, 3, 4, and 5 followed similar trends (fig. 1). Sulfate loadings show the same trends because the water percolation rate was relatively constant. All columns

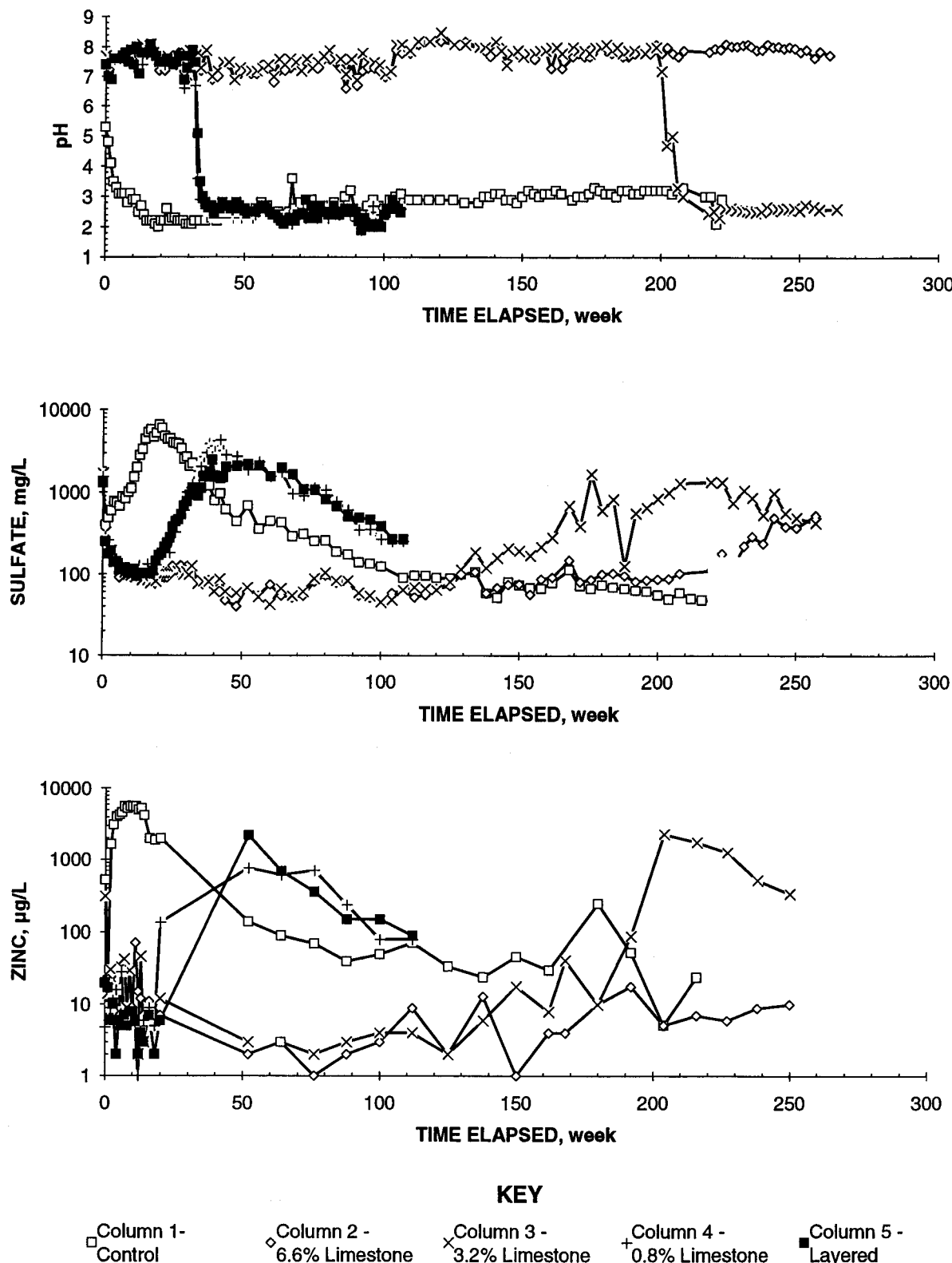


Figure 1. Trends in pH, sulfate, and zinc concentrations in leachates.

showed initially decreasing sulfate concentrations. Concentrations then increased several weeks before pH dropped to between 2 and 3, and peak sulfate release occurred several weeks after the pH dropped.

The observations can be summarized and correlated as follows:

- The time elapsed from a noticeable increase in sulfate concentration to the production of a low pH leachate increased with the proportion of limestone. For columns 4 and 5, 12 weeks elapsed. For column 3, 100 weeks elapsed. Although column 2 did not generate acidic leachate, the time elapsed would be expected to be greater than 180 weeks,
- The time elapsed from release of acidic leachate to peak sulfate concentration was between 9 and 21 weeks for all tests, including the control column,
- The intensity of the sulfate concentration peak decreased with increasing limestone concentration,
- The sulfate concentration peak became less well-defined with increasing limestone concentration, and
- The sulfate decay curve slopes appear to be similar on semilogarithmic graphs, indicating half lives (i.e. time taken to reach half the maximum sulfate concentration) of 5 (control) to 22 weeks.

Sulfate concentrations from column 2 were increasing when the test was terminated. Characteristics of the curve were similar to those of the other tests. Sulfate concentrations had not reached a level that might be expected prior to the onset of fully acidic conditions.

Trends in leachate alkalinity and calcium concentrations were very similar reflecting the dissolution of calcium carbonate. Calcium determinations were most useful for monitoring leaching of limestone because determinations were made regardless of pH. Alkalinity in leachate from column 3 began to increase about 20 weeks after sulfate concentrations increased and peaked at 110 mg/L CaCO₃, just before pH dropped. Calcium concentrations also increased during this period, and peaked at about the same time as sulfate concentrations. Once pH decreased, alkalinity also decreased very rapidly and could not, by definition, be measured once pH dropped to less than 4.5. Alkalinity in leachate from column 2 began increasing about 30 weeks after sulfate concentrations began increasing. Calcium also began increasing.

Dissolved iron was the most significant heavy metal in the column leachates. Sulfate and iron concentrations showed similar trends, although iron varied over a wider range. At low pH (less than 2.9), iron and sulfate concentrations (in mg/L) were comparable. At near neutral pH, iron concentrations were commonly less than the detection limit of 0.03 mg/L. Zinc concentrations (fig. 1) showed similar trends to sulfate. Zinc concentrations began increasing as sulfate increased, long before pH decreased. Peak zinc concentrations tended to precede peak sulfate concentrations by a few weeks.

Characteristics of Column Residues

Column residues were of two types: Columns 1, 3, 4, and 5 (acid generators) contained visibly oxidized (orange-coloured) rock. Column 2 residue was vertically zoned. The upper one third of the column contained oxidized material similar to that in the acid-generating columns. These residues also yielded low paste (de-ionized water) pH. Residue from the lower portion of this column were relatively unweathered (grey-colored), reacted strongly with dilute HCl (indicating readily available NP), and was pH neutral.

Several significant textural features were noted in polished thin sections. In residues from nonacidic columns, abundant fresh pyrite and marcasite grains were observed. These grains showed some in situ replacement by limonite along grain boundaries. By contrast, alteration of pyrite grains varied from negligible to complete in acidic material,

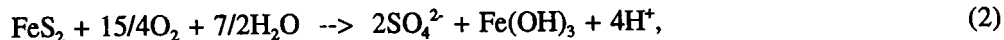
and in situ replacement of sulfide grains by limonite was common. Replacement had taken place along grain edges and along internal fractures and crystal boundaries. In both nonacidic and acidic material, limestone particles appeared fairly fresh and did not have significant limonite rinds. In summary, pseudomorphic (one-for-one replacement) of iron sulfide grains by limonite (primarily goethite, FeOOH) appeared to be common. Coating of limestone grains by transported limonite was not observed.

Acid-base accounting results for residues are summarized in table 1. Reproducibility of duplicate analyses was excellent and confirmed that differences in chemistry between column zones and experiments were significant. Columns 4 (0.8% Limestone concentration) and 5 (layered) yielded very similar results for total sulfur and sulfate. Total sulfur concentrations decreased by about 1.3% over the 2-yr of weathering. All reactive neutralizing material was consumed, as shown by negative neutralization potentials. Column 1 (control) had slightly lower sulfur concentrations after 5-yr of leaching and similarly contained no detectable NP (the negative NP shown in table 1 indicates the presence of soluble acidity). Column 3 yielded slightly greater sulfur concentrations and no NP. Rock from the top part of column 2 (6.6% Limestone) contained higher concentrations of sulfur than any of the other well-oxidized material, and contained a small amount of NP. The deeper, less oxidized material contained about 0.3% less sulfur than at the start of the experiment. NP decreased by 12 kg/mt CaCO₃.

Discussion

Leachate Chemistry

Column leachate chemistries followed a series of stages. Initially, sulfate concentrations were elevated but then decreased rapidly as weathering products accumulated during sample storage were flushed from the columns. During stable pH neutral conditions, the dominant ions in solution were calcium and sulfate. The molar ratio of sulfate to calcium under these conditions was between 0.5 and 1 (fig. 2) which is consistent with general chemical theory for acid generation and neutralization. The usual reaction used to express overall acid generation at pH>3 is



Under strongly acidic conditions, the acidity will be neutralized by CaCO₃:



Under mildly acidic to mildly alkaline conditions, the reaction will be, as follows:

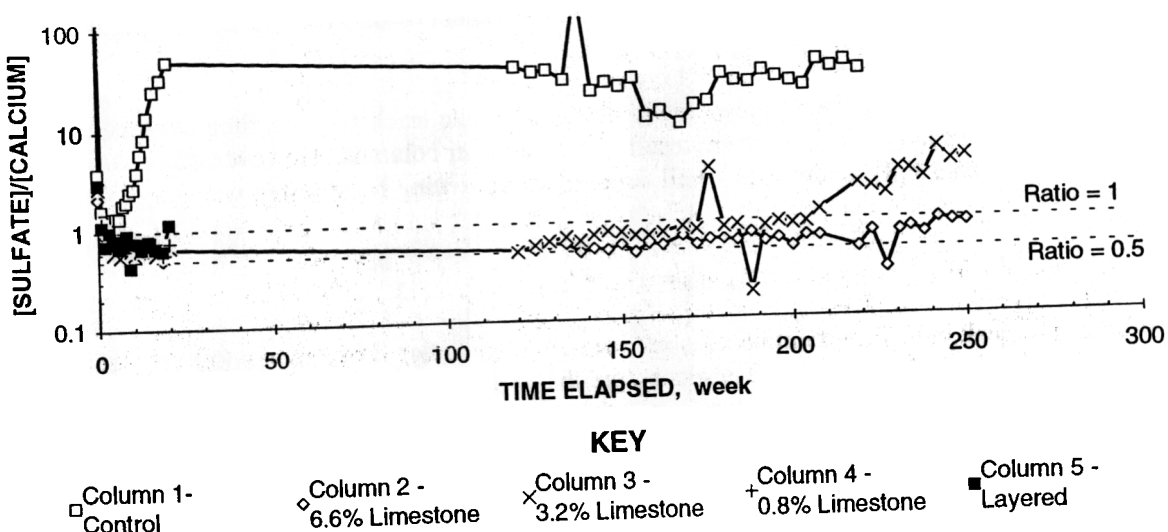
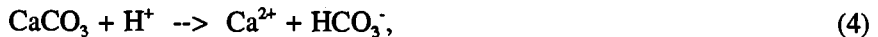


Figure 2. Molar sulfate to calcium ratios.



Under acidic conditions, the molar ratio of sulfate to calcium should be equal to or greater than 1, whereas under less acidic conditions the ratio will be less than 1 owing to the formation of bicarbonate (Cravotta et al. 1990). Several months prior to generation of acidic leachate, this ratio steadily increased and gradually approached 1 (Columns 2 and 3, fig. 2). Once acidic leachate was produced, the ratio passed 1.

Consumption of Alkaline Minerals

Acid-base accounting results for columns generating acid leachate (1,3,4,5) indicated that no neutralization potential remained in the residues. Petrographic observations support the conclusion that all limestone was available for buffering of acidic leachate. Very few limestone fragments were observed in the residues from acidic columns. In the oxidized part of column 2 (highest limestone concentration), remaining limestone fragments were corroded and did not have a thick coating of transported limonite.

The lack of limonite rinds on limestone fragments is consistent with the low iron concentrations in leachate prior to generation of acid and the observed in situ one-for-one replacement of pyrite by limonite (goethite). During overall pH neutral conditions, iron probably remained at the source of oxidation as goethite and was not transported to limestone grains. This result is only observed when limestone and acid generating rock are relatively well mixed. If very acidic conditions are generated in isolated spots, allowing iron to move away from the oxidation site, the resulting iron would precipitate and cement limestone grains. This shows that the availability of calcareous material would probably decrease as the mixture becomes more heterogeneous and may explain the result observed for the layered column. For this column, the higher limestone concentration in the layers did not appear to be available, perhaps owing to cementing once the material above the individual layers became acidic.

Estimation of Alkaline Mineral Requirements

Four of the columns were predicted to be acid generating based on mass-weighted acid-base accounts, and all four columns produced acidic leachate during the course of the experiment. Column 2 (6.6% limestone) did not yield acidic leachate during 5 yr of weathering; however, the upper part of the column was clearly acidic (as shown by low paste pH and negligible neutralization potential), and sulfate and metal concentrations were increasing at the time the experiment was terminated. This column fits the relationship (fig. 3):

$$t_{\text{SO}_4 \text{ increase begins}} = 2.9NP - 25. \quad (5)$$

Although based on only five points (fig. 3), the correlation coefficient ($r=0.991$) is statistically significant with a confidence level of better than 95%.

It is expected that column 2 would have eventually produced acidic leachate. The time required to produce acidic leachate for this column can be estimated from results from the other columns. However, since the time taken for column 1 leachate to become fully acidic is not well defined, the following relationship was determined instead (fig. 3).

$$t_{\text{max SO}_4} = 11e^{0.079NP}. \quad (6)$$

For column 2, the peak sulfate concentration is predicted to occur after 2,600 weeks (50 yr). Leachate pH would be expected to drop to less than 3 about 20 weeks before the peak. The visual progress of the acid generation front suggests a much shorter time frame. If the rate of migration was constant, acid release would have been expected in about 15 yr. The sulfate peak would probably have been at a much lower concentration than for the other columns and would have been poorly defined.

Column no. and Limestone (LS)	NP, kg/mt	Sulfate release increasing, week	Leachate pH<7, week	Sulfate peak, week	Half sulfate peak, week	Sulfate released, % of total
1. Control.....	8	1	1	20	25	62
2. 6.6% LS.....	69	170	-	-	-	11
3. 3.2% LS.....	38	100	200	219	241	50
4. 0.84% LS.....	16	19	31	40	58	61
5. 1.2% LS, layers..	19	19	31	54	72	49

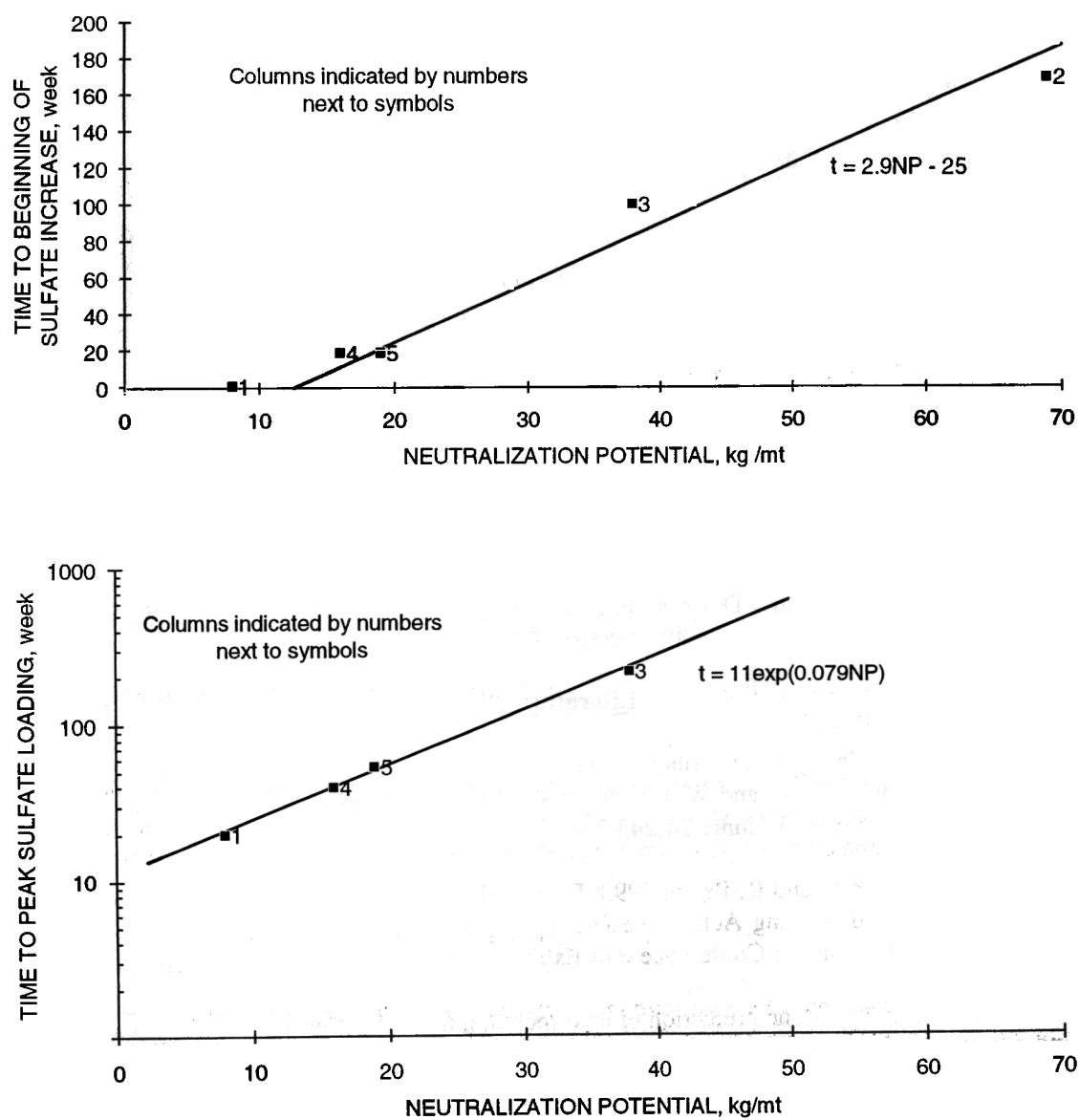


Figure 3 Relationships between beginning of sulfate increase, peak sulfate concentration and time.

The amount of limestone required to neutralize any acid for an indefinite period cannot be estimated from the above relationships since neither converges to a limiting value. However, the molar ratio of sulfate to calcium during the pre-acid leachate phase indicates the release of calcium in proportion to sulfate. The ratio is typically 0.5 to 0.6. As the conventional acid-base account assumes a 1:1 relationship, the actual NP required to prevent acid release is double the amount in column 2 ($NP=69 \text{ kg/mt CaCO}_3$), or 138 kg/mt CaCO_3 .

Mitigation of Metal Release by Calcareous Rock Mixing

Results indicated that under fully alkaline conditions where sulfate production is fairly uniform, metal and arsenic concentrations will remain low and stable. Once sulfate production begins increasing, metal release also increases. Zinc is the first to appear (at about the same time as increasing sulphate concentrations) followed by arsenic and copper (the latter being coincident with low pH conditions). This is consistent with commonly understood relationships between pH and dissolved metal concentrations. It appears therefore that limestone addition will only delay the release of zinc according to relationships of the form of equation (5), but will delay copper release for a much longer period (equation 6).

Conclusions

The following was concluded:

1. The actual quantity of limestone required to prevent acid drainage in perpetuity would probably be at least twice that determined by conventional acid-base accounting provided that the limestone and rock are intimately mixed (not thickly layered) and zinc release is not expected;
2. The time elapsed before marginally acid generating rock released acidity increased exponentially as the quantity of limestone increased; and
3. The time elapsed before sulfate and zinc release began increasing prior to release of low pH leachate was linearly proportional to the neutralization potential.

Acknowledgements

The Mine Environment Neutral Drainage Program (MEND) and British Columbia Acid Mine Drainage Task Force are gratefully acknowledged for granting permission to present this paper.

Literature Cited

Champigny, N. and A. J. Sinclair. 1982. Cinola gold deposit, Queen Charlotte Islands, British Columbia: A Canadian Carlin-type deposit. In Hodder, R.W., and W. Petruk (eds.), Geology of Canadian Gold Deposits, Canadian Institute of Mining and Metallurgy, Special Volume 24:243-254.

Cravotta, C., K. Brady, M. Smith and R. Beam. 1990. Effectiveness of the Addition of Alkaline Materials at Surface Coal Mines in Preventing and Abating Acid Mine Drainage: Part 1. Geochemical Considerations. In Proceedings of the 1990 Mining and Reclamation Conference and Exhibition. (Morgantown, WV, April 23-26, 1990).

Ferguson, K. and K. Morin. 1991. The prediction of acid rock drainage - Lessons from the Database. In Proceedings of the Second International Conference on the Abatement of Acidic Drainage. (Montreal, PQ, September 16-18, 1991).

Sobek, A. A., W. A. Schuller, J. R. Freeman and R. M. Smith, R.M. 1978. Field and laboratory methods applicable to overburden and minesoils. EPA 600/2-78-054, 203 pp.

MITIGATION OF ACID MINE DRAINAGE BY THE POROUS ENVELOPE EFFECT¹

Luc C. St-Arnaud,² Bernard C. Aubé,²
Mark E. Wiseman,³ and Steven R. Aiken⁴

Abstract: A porous envelope effect may occur in ground water systems when mine tailings of low permeability are placed within high-permeability soils. If the permeability contrast between the tailings and the natural soil is large, ground water will flow around the tailings mass rather than through it, and metal leaching will be minimal. A hydrogeological study at the Falconbridge Fault Lake tailings site suggests that conditions for porous envelope containment may be occurring. The tailings have been deposited in a kettle lake formed within glacial outwash sand and gravel. At present, the tailings are mostly above the water table, and surveys using a combination of electromagnetic geophysical methods and monitoring wells did not detect any presence of metals in the ground water. A 2-D finite-element numerical model was used to predict conditions that may occur if the water table would rise within the tailings. The model suggested that the contribution of tailings leachate to the regional ground water system would be small.

Introduction

In 1992, Noranda Technology Centre (NTC) undertook a hydrogeological investigation of the Fault Lake tailings site. The site is unique in that a "porous envelope effect" may be occurring. If this is the case, flow through the tailings mass is low enough, relative to the surrounding, more permeable till, that impact to the ground water by tailings oxidation is insignificant at the regional scale. The specific objectives of the investigation were to analyze the chemical and physical hydrogeology of the site, to delineate areas affected by acid mine drainage (AMD) generated from the tailings, and to verify the presence of the porous envelope effect.

Background

The Fault Lake tailings site is located northwest of the Falconbridge Sudbury operations, approximately 3 km north of Falconbridge and 0.5 km east of the Sudbury Airport. The tailings were deposited between 1965 and 1978 and were produced from the milling of nickel ore in the Sudbury area. Approximately 6.45 million mt of tailings containing as much as 50% pyrrhotite were deposited in a depression of a maximum depth of approximately 30 m. The tailings were contained by dams to the northeast and southeast of the site (referred to as north and south dams). The deposit has an approximate volume of $3.36 \times 10^6 \text{ m}^3$ and a surface area of 22.2 ha (55 acres).

During the spring and fall, ponding occurs at the north dam, south dam, and various berms. The water slowly infiltrates into the tailings and evaporates from the ponds. During the summer, very little ponding has been observed. Tailings in areas where ponding has occurred are soft and gray, while the rest of the tailings are hard and crusty, showing orange traces of oxidation.

¹Paper presented at the International Land Reclamation and Mine Drainage Conference and the Third International Conference on the Abatement of Acidic Drainage, Pittsburgh, PA, April 24-29, 1994.

²Luc St-Arnaud, Program Leader, Hydrogeologist, Bernard Aubé, Environmental Scientist, Noranda Technology Centre, Pointe-Claire, Québec, Canada.

³Mark Wiseman, Supervisor, Environmental Control, Falconbridge Limited, Sudbury Operations, Falconbridge, Ontario, Canada.

⁴Steven Aiken, Hydrogeologist, Elliot Lake, Ontario, Canada.

Surficial Geology

Overburden thickness varies within the studied area, from 36 m to more than 60 m. Overburden mainly consists of coarse to fine glacial outwash sands and gravels, with some large boulders and silt lenses. Kettles, fluvial terraces, discontinuous crevasse fillings, and eskers within the Fault Lake tailings area are evidence of a glacial meltwater channel, partly choked with stranded ice blocks. The small round kettle lakes were formed after the late melting of the stranded ice blocks which were caught among the mass of glacial sediments. The sediments are assembled in longitudinal formations which follow a northeasterly direction.

Investigative Methodology

Installation of Ground Water Monitoring Stations

The routes by which acid water could be transported from the Fault Lake tailings site were examined by electromagnetic surveys (Geomar Inc. 1991 and 1992), and probable seepage routes were identified leaving the tailings site at the base of the north and south dams. Thirteen ground water monitoring stations were placed to sample the ground water in the sediments directly below the tailings deposit and along the seepage routes. In addition, one station (FS-2) was located upgradient of the tailings to characterize background conditions. Figure 1 shows the locations of all the stations and also shows the outline of the original kettle lake as determined from aerial photographs taken prior to tailings deposition. Bedrock in the vicinity of the tailings site was not believed to have an important influence on ground water flow in the area.

Measurements of in situ hydraulic conductivity were conducted at most of the monitoring stations using the "falling-head test." Interpretation of the water level versus time data was conducted using the Hvorslev (1951) method for point piezometers. Ground water was sampled from monitoring wells in December 1992 and in March 1993. Sample pH, temperature, oxidation reduction potential (Eh), and electrical conductance were recorded. Acidified portions were later analyzed for dissolved metal and major ions, and the nonacidified portion was analyzed for chloride. Tailings pore water and the five kettle lakes in the Fault Lake tailings area (fig. 1) were also sampled in 1992.

Results

Physical Hydrogeology

Measurements indicated that the water table is 0 to 2 m below the base of the tailings, except at station FS-6, where there is evidence of a perched water table approximately 8 m above the base of the tailings. At station FS-12, which is the closest to the center of the original kettle lake, the measured water level was approximately 20 m below the tailings surface, near the base of the tailings. The fact that nearly all of the tailings are above the water table is surprising because water was visible in the kettle lake before tailings deposition. Low water infiltration in the tailings and changes in watershed configurations due to nearby quarry excavation are apparently causing the lowering of the water table. Regional ground water flow from the tailings watershed was determined to be northeast toward the small kettle lakes and southeast across the dam.

Hydraulic gradients were calculated for both vertical and horizontal directions. Vertical gradients were near zero at most of the monitoring stations surrounding the tailings deposit. Beneath the tailings deposit, significant vertical gradients indicate percolation. Upward gradients suggest partially confined conditions and/or localized flow paths below the tailings. Horizontal gradients were very small. At the north dam, the horizontal gradient was 0.0002; at the south dam, it was 0.007.

Measured hydraulic conductivities in the natural overburden were highly variable, ranging from 8×10^{-1} cm/s to 2.5×10^{-5} cm/s. The large variations in hydraulic conductivity are explained by the heterogeneity of the soil,

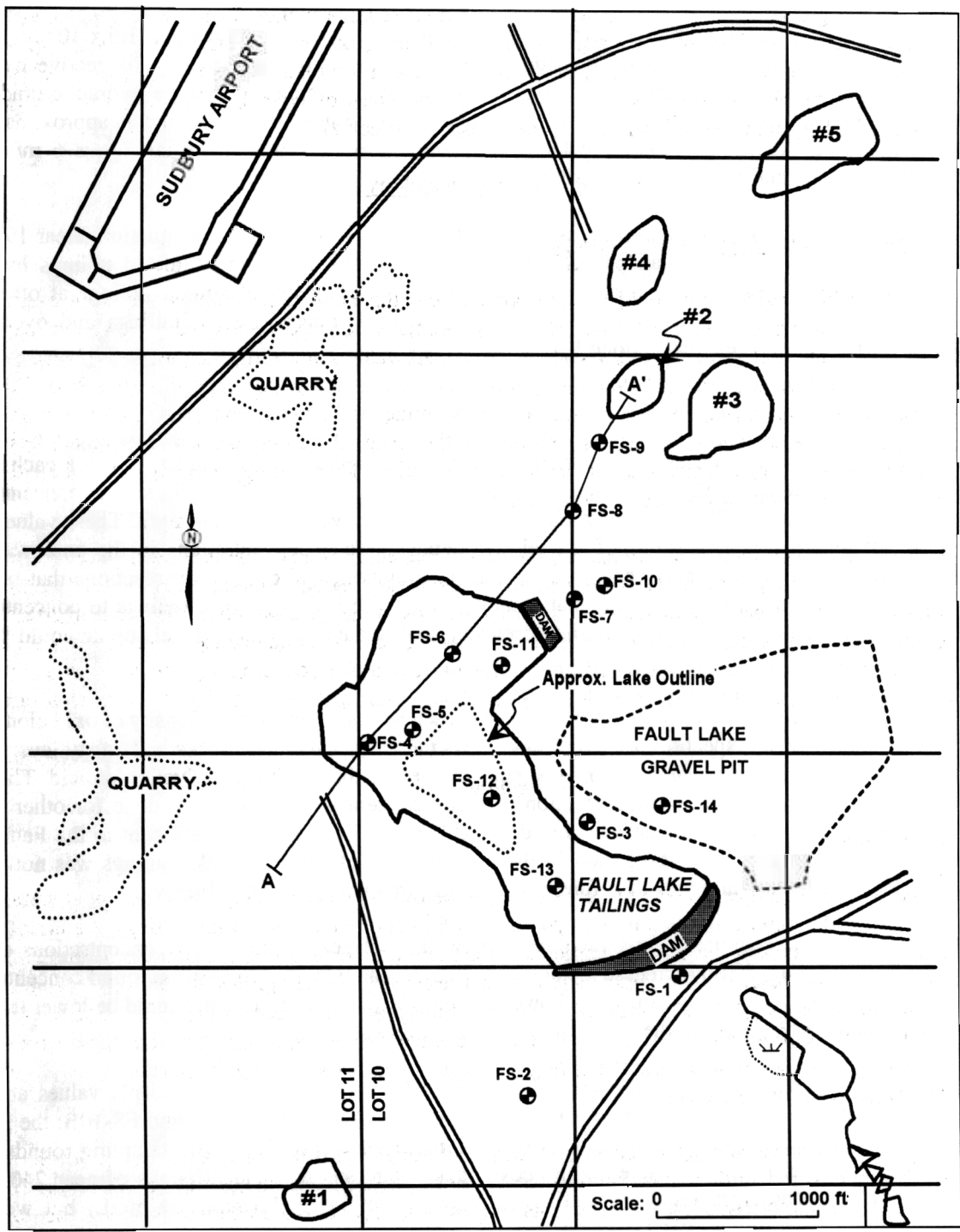


Figure 1. Fault Lake tailings.

typical of ice-contact deposits, which include silts, sands, gravels, and boulders. The higher hydraulic conductivities occur where fast meltwater flows have formed accumulations of well-sorted sands and gravels. The lower hydraulic conductivities occur where glacial abrasion and slow meltwater flows have left finer silts.

The geometric average of all hydraulic conductivity measurements in the overburden is 1.6×10^{-3} cm/s. This value is typical of a clean to silty sand and is considered to be representative of the overall effective hydraulic conductivity of the soils in which the tailings lie. Using the average hydraulic conductivity, a hydraulic gradient of 0.0002, and an estimated effective porosity of 0.30, the calculated velocity north of the tailings is approximately 30 cm/yr. With a horizontal gradient of 0.007, the calculated average velocity south of the tailings is 6 m/yr. This velocity is only approximate, and actual local velocities may vary by a factor of 10.

The hydraulic conductivity of the tailings was estimated using the Kozeny-Carman equation (Bear 1972), an estimated porosity of 0.45, and the median particle diameter, or d_{50} . The resulting estimated tailings hydraulic conductivities averaged 1.2×10^{-5} cm/s, which is consistent with measurements of similar tailings at other sites (Yanful and St-Arnaud 1992, for example). The measured hydraulic conductivities of tailings and overburden materials also agree with previous estimates done by Geocon (1985).

Chemical Hydrogeology

Water extractions were performed on six selected samples collected in November 1992 at each of the monitoring stations located on the tailings. Nickel concentrations ranged from 4 to 644 mg/L, sulfate concentrations ranged from 3,041 to more than 84,600 mg/L, and total iron concentrations were 0.5 to 466 mg/L. These values show evidence of sulfide oxidation within portions of the tailings deposit. Metal concentrations in the pore water are strongly influenced by downward water movement, chemical precipitation, and dissolution reactions that occur in the tailings mass. These effects seem to have attenuated nickel in the deeper parts of the tailings to concentrations of 5 to 8 mg/L. Thermodynamic calculations done on porewater quality data suggested nickel sulfate could be near saturation.

Differences in measured metal concentrations could be caused by variations in the intensity of oxidation across the surface of the tailings. Visual inspection of the tailings shows the development of cracks and crusty layers at the surface, which could locally influence water and oxygen entry as well as the resulting production of acid. Thorough investigations of the geochemical sources and evolution of metal concentrations have been done for other sulfide tailings sites (Blowes et al. 1988) and for the Falconbridge main pyrrhotite tailings site adjacent to the Fault Lake site (Nicholson and David 1991). The investigation of the geochemistry of the Fault Lake tailings was not part of the objectives of the present study and was therefore not pursued further than described above.

Background ground water monitoring station FS-2 showed a pH near 7 and nickel concentrations of 0.01 mg/L, iron 0.03 mg/L, and sulfate 30 mg/L. These metal concentrations can be accepted as background concentrations for ground water at the site since a second sampling showed similar results. Background pH could be lower than that measured at FS-2 (as low as 6) owing to the infiltration of acidic rainwater.

Ground water sampled near the tailings site in December 1992 and March 1993 had pH values above 6. Above-background concentrations of nickel were measured in wells FS-3A, FS-3B, FS-9C, and FS-10B; the highest of these concentrations was 0.5 mg/L (at FS-10) and was measured during only one of the sampling rounds. Only at FS-3 were the higher nickel levels associated with above-background sulfate concentrations of near 240 mg/L. Above-background sulfate concentrations were also encountered at station FS-1 (max 339 mg/L) but were not associated with any above-background metal concentrations.

Sampling results suggest that metal concentrations are not high enough to affect ground water quality. This is also suggested by the results of surface water quality sampling, which do not show the presence of any metal above background concentrations.

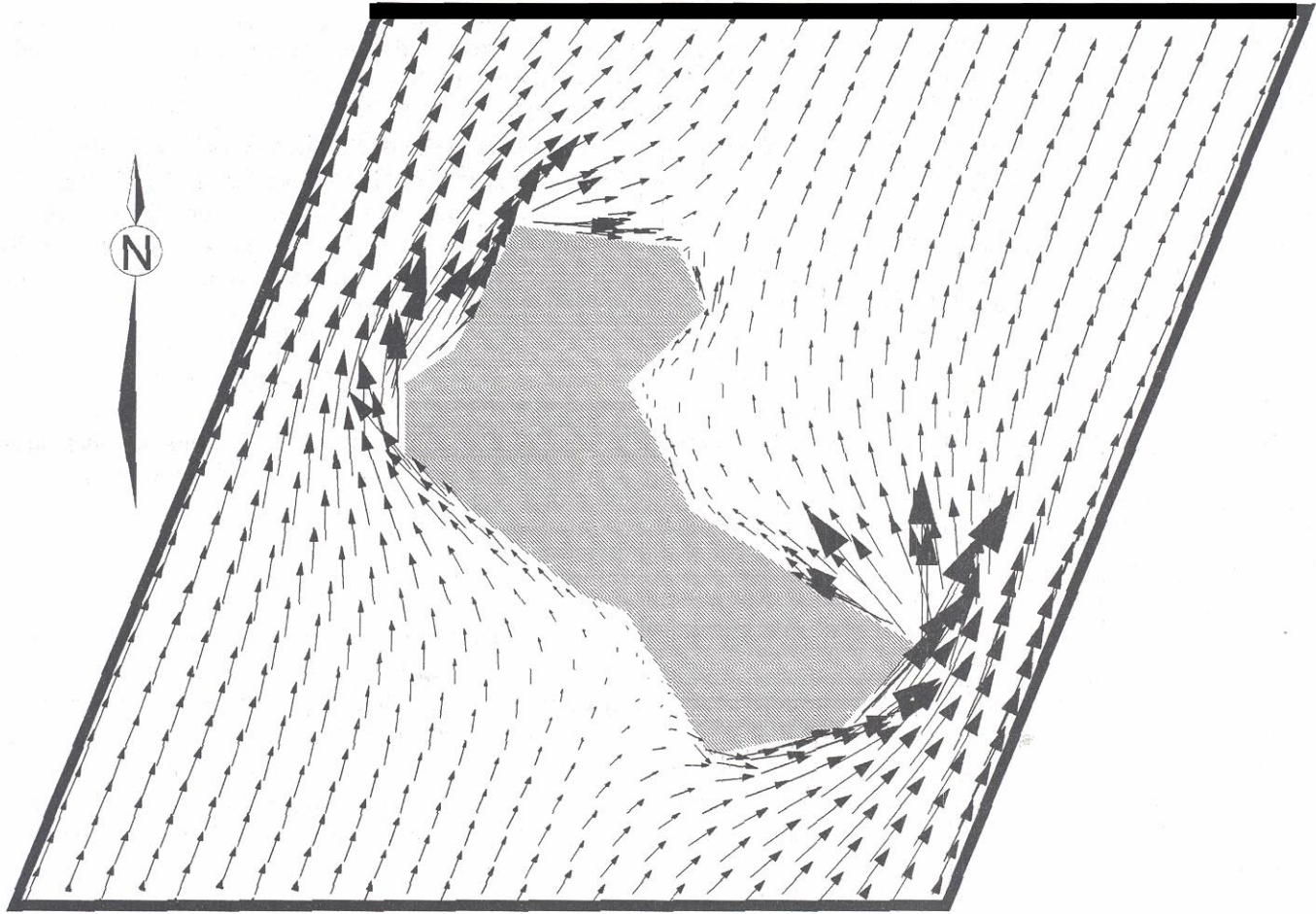


Figure 2. Plan **view** modeling results.

Ground Water Flow Modeling

Modeling Procedure

Ground water flow around the tailings was simulated using the saturated-unsaturatedflow modeling program SEEPN (GEO-SLOPE International 1992). In order to determine the **flownet**, SEEPN requires the definition of i) a domain (finite-element grid), ii) soil hydraulic conductivities, and iii) boundary conditions.

Two models were defined in order to obtain a quasi-three-dimensional perspective of the ground water flows in the Fault Lake tailings area. The first model was a plan model and was defined as a rectangle with the long edges parallel to the main flow direction inferred from previous analysis. This model was conceptual only, representing the flow of water directly beneath the soil surface as affected by the hydraulic conductivity contrast between the tailings and the surrounding sediments. This did not include the effects of topography or infiltration.

The second model was a cross section across stations FS-4 to FS-9 (A-A' in fig 1). The model domain started southwest of **piezometer** FS-4, extended northeast of FS-9, and passed through FS-6 and FS-8. Elevations were taken from the monitoring well data where possible; otherwise, the topographic map was used. Representative hydraulic conductivities (K) for the soils and tailings were derived from the geometric mean of the field measurements, as described earlier.

Constant-head boundary conditions were defined at both ends of the model domains. In the first model, the constant-heads were set equal to the elevation of the nearest lakes: lake #1 in the south and lake #3 in the north.

In the second model, a water table elevation slightly higher than that measured at FS-4 was used at A; for A', the elevation of lake #2 was taken from the topographic map. The infiltration flux across the top boundary was determined using previous estimates from Yanful et al. (1993) obtained using the HELP (Hydrologic Evaluation of Landfill Performance) computer program of Shroeder et al. (1984). Different fluxes were used in the SEEP/W modeling, depending on the slope and nature of the ground surface. The tailings surface infiltration was set to 200 mm/yr, sloped till 250 mm/yr, and flat till 350 mm/yr. It was determined that infiltration into the till would be higher than that into the tailings since the hydraulic conductivity is higher and the water table is low. This would cause precipitation to be absorbed by the till and transferred away from the surface (to the water table), thereby limiting evaporation. On the tailings, evaporation is enhanced by surface ponding, thereby reducing infiltration.

Modeling Results

Flow vectors for the first model are shown in figure 2. The flow vectors illustrate the direction of flow, with their length being proportional to the flux. The figure clearly shows how the water would flow mainly in the till and around the tailings because of the higher hydraulic conductivity of the till. Figure 2 is only a conceptual illustration of actual conditions since this modeling procedure is highly simplified. For realistic results in a plan view, topography, depth of soils, and infiltration would need to be included into a three-dimensional modeling program.

Figure 3 depicts the flow characteristics for the cross-sectional model. The figures indicate that the horizontal flow is predominantly in the till and does not enter the tailings. The only water flowing through the tailings is the water that infiltrates from precipitation.

The flow vectors in figure 3 show a ground water divide left of the tailings (southwest). Although the general flow was calculated to be toward the northeast, it is possible that local gradients occur that cause some water to travel southwest. Such digression in the flow could be caused by manmade changes, such as the gravel pits in the area. From aerial pictures taken before tailings deposition, it is known that this area was once a lake. The fact that the water table is now below what used to be the lakebed suggests that local excavation may have greatly affected regional ground waters. A second influence to the water level is the tailings, which, by decreasing infiltration and promoting evaporation, reduce recharge to the aquifer. Other human disturbances, such as the building of roads, may have affected watersheds and ground water flow directions. It is also possible that the present conditions are temporary, and that the water table could eventually return to previous levels.

To verify the effects that would occur if the water table were to rise into the tailings and saturate the bottom portion of the impoundment, the constant-head boundary functions at either end of the section were raised. The results of this simulation showed that, although the bottom 5 m of the tailings are saturated, the flow within the tailings remains insignificant. This suggests that the increase in metal loading in the ground water due to the water table rise would not be important.

The use of a 2-D flow model to assess the conditions on the Fault Lake site has inherent limitations. In particular, any quantification of flow volumes is affected by the fact that all the water is assumed to move only in the reference plane, while in reality water also moves across the plane. Model predictions based only on ground water flow can also lead to overestimation of chemical loadings, since metal transport is usually slower than water velocity owing to chemical attenuation. The flow model can, however, be used to predict the worst-case scenario where no chemical attenuation takes place. Predictions that account for chemical attenuation are complex and were not part of the objectives of the present study.

Discussion

The glacial sediments surrounding the Fault Lake tailings site are characterized by their elongated formation and relatively high bulk hydraulic conductivities. This creates a flow system with a relatively flat and deep water table. Several favorable factors contribute to limit the observed metal concentrations downgradient of the tailings. These factors and their probability of occurring elsewhere follow:

1. Hydraulic conductivity contrast: Sediments of high hydraulic conductivities such as sands and gravels occur commonly in Canada. The ice-contact deposits surrounding the Fault Lake area possess a high average hydraulic conductivity, but are also characterized by a high variability due to the process by which they were deposited. Other sands and gravels may be more uniform, showing less heterogeneity in hydraulic properties and possibly a higher bulk hydraulic conductivity. As for tailings, measurements at several sites by Blowes et al. (1988) and Yanful and St-Arnaud (1992) have yielded values close to 10^{-5} cm/s, as measured at the Fault Lake tailings. Large hydraulic conductivity contrasts between tailings and surrounding sediments are therefore possible.

2. Deep water table: The water table in well-drained sand and gravel formations in temperate climates will usually be far below the ground surface. The depth to water table is also largely affected by topographical features. The hummocky terrain surrounding the Fault Lake site is largely controlled by the occurrence of the kettle lakes. In other similar glacial outwash areas, the coarse glacial deposits are commonly elevated, and deep water tables can result, depending on bedrock topography.

3. Limited infiltration: Infiltration of water through tailings surfaces is usually less than through natural soils. This is due to the relatively low bulk hydraulic conductivity of the tailings, the high potential for evaporation at the tailings surface, and the formation of dense crusts which can further reduce conductivity at the tailings surface. At the Fault Lake tailings site, infiltration could be reduced by encouraging runoff, thus preventing ponding along the dams.

4. Dilution by regional ground water flow: Large glacial outwash sediment formations normally have high ground water discharges, which are less susceptible to degradation by point contamination sources. In the case of the Fault Lake site, results from the second model (A-A' cross section) suggest that flow upstream of the tailings site would not be very large. The occurrence of much larger regional flow systems at other sites is possible.

5. Chemical attenuation: Some chemical attenuation in the form of precipitation and adsorption reactions occurs in most tailings. The degree to which these reactions take place depends on geochemical and mineralogical factors, in particular those that influence the neutralization potential of the tailings. Chemical attenuation in the Fault Lake tailings is suggested by the tailings pore water data and could also occur within the natural overburden deposits.

All five factors outlined above contribute to create the porous envelope effect; these factors could probably be present at other locations near mine sites. Tailings deposition in these types of environments could be done with little effect on ground water quality, if thorough site evaluations are performed and appropriate control is enforced at the time of deposition.

Conclusions

1. The piezometric elevations throughout the Fault Lake site, combined with lake elevations, suggest that the regional direction of subsurface flow is toward the northeast, along with the alignment of the kettle lakes. Some subregional flow systems could be moving ground water in other directions.
2. The base of the tailings is at the same level or higher than the water table across most of the site. Low water infiltration in the tailings and changes in watershed configurations due to nearby quarry excavation are suggested as causes for the apparent lowering of the water table.

3. The average bulk hydraulic conductivity of the soil surrounding the tailings is estimated at 1.6×10^{-3} cm/s. The hydraulic conductivity of the tailings was estimated using grain size correlations at 1×10^{-5} cm/s. These values agree with previous estimates.
4. Analysis of tailings pore water showed elevated values of nickel, iron, and sulfate, indicating the presence of sulfide oxidation products within portions of the tailings deposit. Metal concentrations are attenuated in the deeper parts of the tailings. Heterogeneity in measured metal concentrations could be caused by variations in the intensity of oxidation across the surface of the tailings due to surface effects such as ponding and cracking.
5. Water quality sampling in monitoring wells outside the tailings did not show any evidence of above-background metal concentrations, which suggests that leaching of metals from the tailings would be minimal. This is also suggested by the results of water sampling in nearby lakes.
6. Two-dimensional ground water models showed that the flow is diverted around the tailings mass owing to the hydraulic conductivity contrast between the tailings and the surrounding sediments. The models also showed that flushing of the tailings by ground water should not contribute significantly to the regional ground water flow system under present water table conditions, as well as under conditions of moderate rise in water table level.

Factors that contribute to limit metal concentrations downgradient of the Fault Lake tailings are:

- the large hydraulic conductivity contrast between the tailings and the surrounding sediments.
- the low position of the water table relative to the tailings bottom.
- the limited infiltration through the surface of the tailings.
- the dilution of metals flushed from the tailings by water flowing around and below the tailings.
- chemical attenuation of metals in the tailings and overburden.

8. These factors could probably be present at other locations near mine sites. Tailings deposition could be done at these sites with little effect on ground water quality if thorough site evaluations are performed and appropriate control is done at the time of deposition.

Acknowledgements

This project was funded by Falconbridge Limited and by the Ontario Ministry of Northern Development and Mines as part of the MEND program. Acknowledgements are owed to M. Woyshner for reviewing the paper and to B. Michelutti and B. Mikkila of Falconbridge Ltd. for providing useful comments and site information.

Literature Cited

- Bear, J. 1972. Dynamics of fluids in porous media. American Elsevier, New York. p. 161-167.
- Blowes, D. W., J. A. Cherry, and E. J. Reardon. 1988. The rate of geochemical evolution of the Heath Steele mine tailings, New Brunswick. p. 5-17. In C. L. Lin (ed.), Proceedings of the International Ground water Symposium on Hydrogeology of Cold and Temperate Climates and Hydrogeology of Mineralized Zones. International Association of Hydrogeologists, Canadian National Chapter, Halifax, NS.
- Felmy, A. R., D. C. Girvin, and E. A. Jenne. 1984. MINTEQ—A computer program for calculating aqueous geochemical equilibria, U.S. Environmental Protection Agency, Athens, GA, EPA-600/3-84-032.
- Freeze, R. A. and J. A. Cherry. 1979. Groundwater. Prentice-Hall, Inc., Englewood Cliffs, NJ.
- GEOCON. 1985. Unpublished data submitted to Falconbridge Limited.

- Geomar Inc. 1991. EM survey, Falconbridge operations, Fault Lake, Falconbridge, Ontario, Canada.
- Geomar Inc. 1992. TEM survey, Falconbridge operations, Fault Lake, Falconbridge, Ontario, Canada.
- GEO-SLOPE International. 1992. SEEP/W version 2 user manual. Geo-Slope International Limited, Calgary, AB, Canada.
- Hvorslev, M. J. 1951. Time lag and soil permeability in ground water observations. U.S. Army Corps Engrs. Waterways Exp. Sta. Bull. 36, Vicksburg, Ms.
- International Water Supply Ltd. 1971. Department of Transport ground water investigation, Sudbury Airport.
- Nicholson, R. N. and D. J. David. 1991. Preliminary hydrogeological investigation of the Falconbridge new tailings impoundment: fall 1990. Final report. Waterloo Centre for Ground water Research report submitted to Falconbridge Limited.
- Schroeder, P. R., J. M. Morgan, T. M. Walski, and A. C. Gibson. 1984. The hydrologic evaluation of landfill performance (HELP) model. U.S. Environmental Protection Agency, Office of Solid Waste and Emergency Response, Washington, DC.
- Yanful, E. K. and L. C. St-Arnaud. 1992. Migration of acidic pore waters at the Waite Amulet tailings site near Rouyn-Noranda, Quebec, Canada. Canadian Geotechnical Journal, Vol. 29: 466-476.
- Yanful, E. K., M. R. Woyshner, and B. C. Aubé. 1993. Field evaluation of the effectiveness of engineered soil covers for reactive tailings. Report for MEND, DSS contract 23440-0-9061/01-SQ.

POTENTIAL MICROENCAPSULATION OF PYRITE BY ARTIFICIAL INDUCEMENT OF FePO_4 COATINGS

V.P. Evangelou

Abstract: A novel coating methodology was developed to prevent pyrite oxidation in mining "waste." The mechanism of this coating technology involves leaching mining "waste" with a phosphate solution containing hydrogen peroxide (H_2O_2); when this solution reaches pyrite surfaces, H_2O_2 oxidizes the surface portion of pyrite and releases Fe^{3+} so that iron phosphate precipitates and forms a passive coating on pyritic surfaces. This study demonstrated that iron phosphate coatings on pyritic surfaces could be established with a solution containing as low as 10^{-4} mol/L phosphate and 0.027 mol/L H_2O_2 and that the iron phosphate coating could effectively protect pyrite from oxidizing further. Development of this coating methodology could mean solution to production of acid mine drainage from certain types of mine "waste." Further investigations are being carried out to extend this methodology to practical use.

Introduction

Pyrite oxidation in mining "waste" or overburden is considered as the main cause for the production of acid mine drainage (AMD). The need to prevent AMD formation has triggered numerous investigations into the mechanisms of pyrite oxidation and its prevention (Singer and Stumm, 1970; Silverman, 1967; Nordstrom, 1982; Kleinmann et al., 1981; Ziemkiewicz, 1990).

It has been reported that pyrite in mining wastes or coal overburden is initially oxidized by the atmospheric O_2 , producing H^+ , SO_4^{2-} , and Fe^{2+} (Nordstrom, 1982). The Fe^{2+} produced can be further oxidized by O_2 into Fe^{3+} , which in turn hydrolyzes into amorphous iron hydroxide and releases additional amounts of acid into the environment (Nordstrom, 1982). In this initial stage, pyrite oxidation in pyritic "waste" is a relatively slow process (Ivanov, 1962). As acid production continues and the pH in the vicinity of the pyritic surfaces drops below 3.5, the formation of ferric oxide is hindered and the activity of free Fe^{3+} in solution increases. Under these conditions, the oxidation of pyrite by Fe^{3+} becomes the main mechanism for acid production in mining wastes since Fe^{3+} can oxidize pyrite at a much faster rate than O_2 (Singer and Stumm, 1970). Meanwhile, at low pH, an acidophilic, chemoautotrophic, iron-oxidizing bacterium, *Thiobacillus ferrooxidans*, flourishes; it can catalyze and accelerate the oxidation of Fe^{2+} into Fe^{3+} by a factor larger than 10^6 (Singer and Stumm, 1970) and thereby effectively recycle the iron released from pyrite as a major oxidant of pyrite or as an electron conductor between FeS_2 and O_2 (Kleinmann et al., 1979). *Thiobacillus ferrooxidans* is thus considered to be primarily responsible for the rapid oxidation of pyrite in mining wastes at low pH (Nordstrom, 1982).

So far the approaches to preventing pyrite oxidation are mainly based on the above mechanisms and are aimed at eliminating Fe^{3+} from pore waters. These approaches include the use of phosphate to precipitate Fe^{3+} in the insoluble form as FePO_4 (Ziemkiewicz, 1990) and the application of bactericides to inhibit the oxidation of Fe^{2+} into Fe^{3+} (Kleinmann et al., 1981). Both approaches have shown a certain degree of success in preventing pyrite oxidation and acid production in pyritic "waste"; however, they both have two weaknesses-they are costly and have a short span of effectiveness. The main reason for the failure of these methods is that the surfaces of pyrite particles in mining "waste" are still exposed to the atmospheric O_2 after treatment; as Fe^{2+} accumulates and *Thiobacillus ferrooxidans* repopulates on pyritic surfaces, pyrite oxidation by Fe^{3+} and acid production is initiated (Kleinmann and Crerar, 1979). To completely prevent pyrite oxidation, it appears essential to block the access of the atmospheric O_2 to pyritic surfaces.

The purpose of this study was to examine the feasibility of creating an iron phosphate coating on pyrite surfaces to prevent pyrite oxidation. The basic hypothesis for this coating approach was that by leaching pyritic mining "waste" with a phosphate solution containing a low concentration of H_2O_2 , the Fe^{3+} released from pyrite by H_2O_2 will react with phosphate to form a passive FePO_4 coating on pyrite surfaces. Thus, at the expense of a small fraction of pyrite, oxidation of pyrite and production of acid could be prevented.

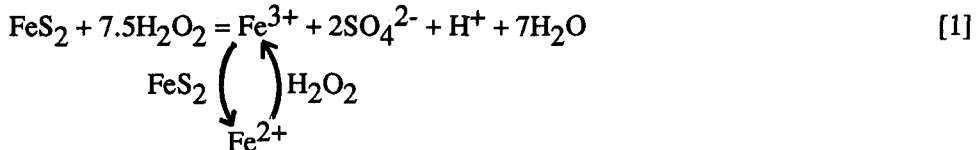
Theory

Pyrite Oxidation by H_2O_2

Pyrite oxidation by H_2O_2 can be described as follows (Huang and Evangelou, 1992):

Paper presented at the International Land Reclamation and Mine Drainage Conference and the Third International Conference on the Abatement of Acidic Drainage, Pittsburg, PA, April 24-29, 1994.

V. P. Evangelou, Department of Agronomy, Univ. of Kentucky, Lexington, KY 40546-0091.



According to equation 1, pyrite oxidation is an autocatalytic process because one of the oxidation products, Fe^{3+} , can also oxidize pyrite. The rate law corresponding to this oxidation mechanism can be written as

$$-\frac{dM}{dt} = (k_1[\text{H}_2\text{O}_2] + k_2[\text{Fe}^{3+}])KM,$$
[2]

where M is the number of moles of pyrite in the system at any time t. $[\text{H}_2\text{O}_2]$ and $[\text{Fe}^{3+}]$ refer to concentrations of H_2O_2 and Fe^{3+} , while k_1 and k_2 refer to the rate constants of H_2O_2 and Fe^{3+} , respectively; K stands for the specific surface of pyrite.

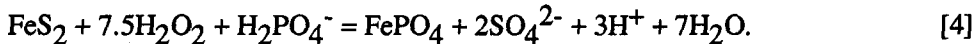
By moving M in equation 2 to the left-hand side, integrating with respect to M and expressing it as log to the base 10, equation 2 becomes

$$-\frac{d\log M}{dt} = (k_1/2.3[\text{H}_2\text{O}_2] + k_2/2.3[\text{Fe}^{3+}])K.$$
[3]

According to equation 3, the first-order plot of $\log M$ versus t will be curvilinear even if $[\text{H}_2\text{O}_2]$ is kept constant. Whether the plot concaves down or up depends on whether the Fe^{3+} concentration in the system increases or decreases with time. However, if Fe^{3+} is prevented from oxidizing pyrite and $[\text{H}_2\text{O}_2]$ is kept constant, the plot will be a straight line.

Pyrite Oxidation by H_2O_2 in the Presence of Phosphate

Pyrite oxidation by H_2O_2 in the presence of phosphate can be described by:



The iron phosphate formed can precipitate either as a discrete phase or as a coating on pyritic surfaces, depending on the degree of the supersaturation of the solution on pyritic surfaces with respect to iron phosphate (Huang and Evangelou, 1992). If the degree of supersaturation is relatively low, the iron phosphate might not precipitate instantly and thereby exist as a discrete phase. In this case, equation 3 becomes

$$-\frac{d\log M}{dt} = Kk_1/2.3[\text{H}_2\text{O}_2].$$
[5]

This equation implies that the precipitation of iron phosphate as a discrete phase is characterized by the linear first-order plot of $\log M$ versus t if $[\text{H}_2\text{O}_2]$ is kept constant.

If the degree of supersaturation with respect to iron phosphate is high, iron phosphate will precipitate as a coating on pyritic surfaces. The rate of pyrite oxidation should be smaller than that predicted by equation 5 as pyrite oxidation is not only surface chemical reaction-controlled but also coatings-controlled. In this case, the kinetics of pyrite oxidation would be described by the shrinking core model (Huang and Evangelou, 1992; Nicholson et al., 1989):

$$t = 1/(Ds'C)\{1 - 3(1-X)^{2/3} + 2(1-X)\} + 1 / (Ks'C) \{ 1 - (1-X)^{1/3}\}$$
[6]

where t is the time required for a specific fraction (X) of pyrite to oxidize in the system and C is the concentration of H_2O_2 in the bulk solution. Ds' is the apparent diffusion coefficient for H_2O_2 through FePO_4 coatings and Ks' is the first-order rate constant with respect to pyrite. The first term in equation 6 describes the effect of accumulation of iron phosphate precipitates on pyritic surfaces on the rate of pyrite oxidation. The second term describes the first-order kinetics with respect to pyrite itself. Note: The second term in equation 6 is the same as equation 5.

Materials and Methods.

The sample used in this study was a pyritic shale with 6.5% pyrite. The shale sample was pulverized, passed through a 60-mesh sieve, and stored in a plastic bag. Part of the pulverized sample was used to separate pyrite using a heavy liquid, 97% tetrabromoethane. The separated pyrite particles were washed with 4 mol/L hydrofluoric acid to remove silicate and iron oxides and then rinsed repeatedly with nitrogen-purged distilled water. The cleaned sample

was then dried and stored in a vacuumed desiccator. X-ray diffraction analysis indicated that the separated sample was pure pyrite and free of any crystalline impurities.

To prove the feasibility of coating pyrite with iron phosphate, we leached a mixture of 50 mg of the separated pyrite sample and 500 mg of 140-mesh sand with the following three solutions, using a chromatographic column (fig. 1) and a peristaltic pump at a flow rate of 0.5 mL/min and a temperature of 40°C: 0.147 mol/L H₂O₂, 0.147 mol/L H₂O₂ with 0.013 mol/L disodium ethylenediamine tetraacetate (EDTA), 0.147 mol/L H₂O₂ with 0.01 mol/L KH₂PO₄. All three solutions contained 0.1 mol/L NaCl as background electrolyte and were adjusted to pH 4 with 0.01 mol/L HCl. At pH 4, it was expected that the Fe³⁺ produced during pyrite oxidation was either completely complexed by EDTA or precipitated by phosphate as FePO₄. The pyrite-sand mixture in the column was pressed into a disc with a diameter of 10 mm and a thickness of 3 mm and preleached with 50 mL of 2 mol/L HCl to guarantee removal of free FeSO₄ and iron oxides. The leachate from the column was collected at 20-min. intervals with a fraction collector.

At the end of leaching, the residual pyrite particles in the pyrite-sand mixture were separated with 97% tetrabromoethane. The residual pyrite particles were further washed with acetone and dried in a vacuumed desiccator. The surface status of pyrite particles was then examined using scanning electron microscopy and diffuse reflectance infrared spectroscopy.

To determine the effectiveness of the coating approach in preventing pyrite oxidation, two columns with a mixture of 0.5 g of the pulverized shale and 0.5 g of 140-mesh sand were leached first with 50-mL of 2 mol/L HCl to expose pyritic surfaces and then with 500-mL of pH 4 solutions containing 0.1 mol/L NaCl, 10⁻⁴ mol/L KH₂PO₄, and 0.053 mol/L H₂O₂ to coat pyrite particles. The leachates were collected in a 500-mL bottles. One of the columns was leached again with 50 mL of 2 mol/L HCl to remove the iron phosphate coating. Both columns were then subjected to leaching at 40°C with a pH 4 oxidizing solution containing 0.1 mol/L NaCl and 0.088 mol/L H₂O₂ to test the effectiveness of the coating in preventing pyrite oxidation. Leachates were collected at 20-min intervals using a fraction collector. All the leaching experiments were conducted using the chromatographic column (fig. 1) at 40°C and a flow rate of 0.5 mL/min.

Sulfate concentration in the leachates was measured using turbidometry with BaCl₂. The amount of pyrite remaining in the column was calculated according to the FeS₂-SO₄ stoichiometry and the extent of pyrite oxidation was expressed as percent of remaining pyrite versus time.

Results and Discussion

Kinetics of Pyrite Oxidation During Leaching

Figure 2 shows the first-order plot of log (100 x M/M₀) versus t (M₀ = original amount of pyrite, and M = amount of unreacted pyrite at any time t) for the data of pyrite oxidation when pyrite was leached with the three solutions listed in the caption. During leaching with 0.147 mol/L H₂O₂, pyrite rapidly oxidized and by the end of leaching, 70% of pyrite was oxidized. The first order plot was curvilinear and concaved up. Since the total volume of pores in the pyrite-sand column was small (the total volume of the column was 0.058 cm³), the concentration of H₂O₂ used was high, and the residence time of the leaching solution within the column was low, it was assumed that H₂O₂ concentration in contact with pyritic surfaces was always constant. With this assumption, the curvature of the first order plot can be attributed to oxidation of pyrite by Fe³⁺ (equation 3). The analysis of the iron in the leachate indicated that the amounts of the soluble Fe³⁺ released from pyrite decreased dramatically with time, and approximately 50% of iron released from pyrite precipitated as iron hydroxide within the column by the end of leaching (fig. 3A).

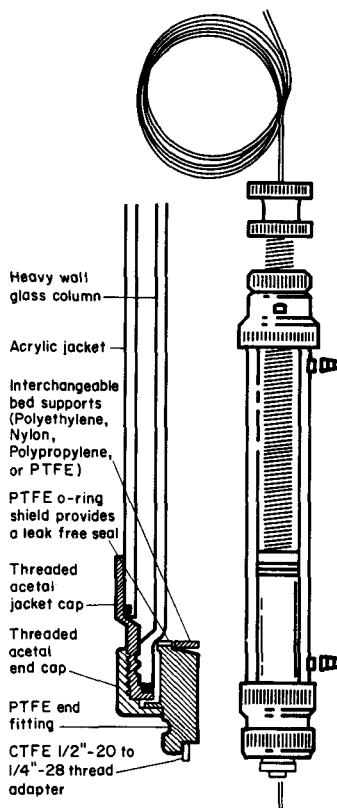


Figure 1. Chromatographic column for pyrite leaching experiments.

When pyrite was leached with the solution containing 0.147 mol/L H_2O_2 and 0.013 mol/L EDTA, the rate of pyrite oxidation decreased, especially during the initial stage of leaching, but it did not stop; at the end of leaching, approximately 65% of pyrite was oxidized, a value close to that for being leached with 0.147 mol/L H_2O_2 . The first order plot was a straight line (fig. 2, curve B). This indicated that pyrite oxidation by Fe^{3+} had been completely inhibited by EDTA (equation 3). Analysis of iron in the leachates confirmed that 100% of the iron released from pyrite was instantly flushed out of the column (fig. 3, curve B).

When the pyrite was leached with the solution containing 0.147 mol/L H_2O_2 and 10^{-2} mol/L KH_2PO_4 , almost 99% of the iron released from the pyrite was precipitated by phosphate (fig. 3, curve C). The precipitation of iron as $FePO_4$ might influence the rate of pyrite oxidation via two mechanisms: (1) by inhibiting the oxidation of pyrite by Fe^{3+} or (2) by forming a passive coating. As shown in figure 2, pyrite oxidation during leaching with the solution containing 0.147 mol/L H_2O_2 and 0.01 mol/L KH_2PO_4 was much slower than that during leaching with the solution containing 0.147 mol/L H_2O_2 and 0.013 mol/L EDTA (fig. 2, curve C). Before 300 min, the first-order plot was nearly parallel to that of EDTA treatment. This indicates that at the initial stage of leaching phosphate inhibited oxidation of pyrite by Fe^{3+} by precipitating Fe^{3+} as $FePO_4$, but not all the iron phosphate had precipitated as coating. After 300 min of leaching, pyrite oxidation nearly stopped. At the end of leaching, more than 70% of pyrite was preserved. The above results clearly suggest that by leaching with the phosphate solution containing H_2O_2 , we can establish an iron phosphate coating on pyrite surfaces at the expense of surface portions of pyrite particles.

The growth of iron phosphate coatings on pyrite surfaces during leaching with phosphate solution containing H_2O_2 can be well explained with the shrinking core model. As indicated in the Theory section, the second term in equation 6 represents first-order kinetics with respect to pyrite. During leaching with the solution containing H_2O_2 and EDTA, pyrite oxidation by Fe^{3+} was inhibited and no coatings were supposed to form. Thus, the rate of pyrite oxidation by H_2O_2 is of the first order with respect to pyrite. This was clearly confirmed by the linearity of the plot of t versus $\{1-(1-X)^{1/3}\}$ (fig. 4) (deviation from straight line at around 700 min is believed to be due to the failure of the linear relationship between the surface area and the mole number of the remaining pyrite (Turner, 1960)). With the apparent first-order rate constant obtained from the plot in figure 4, we expressed the data of pyrite oxidation during leaching with the solution containing 0.147 mol/L H_2O_2 and 0.01 mol/L KH_2PO_4 as a plot of $t-1/(K_s'C)\{1-(1-X)^{1/3}\}$ versus $\{1-3(1-X)^{2/3} + 2(1-X)\}$ (fig. 5). The values of $t-1/(K_s'C)\{1-(1-X)^{1/3}\}$ represent the extra time required for H_2O_2 to oxidize a given fraction of pyrite due to iron phosphate coatings. As shown in figure 5, the plot followed a straight line after 200 min of leaching. The shrinking model requires that all the iron phosphate formed precipitate as a coating on pyritic surfaces. The deviation from linearity before 200 min indicates that some iron phosphate did not precipitate as coating. Part of the reason is that the concentration of acid produced by pyrite oxidation was relatively high during the initial stages of leaching (pH of the leachates was 2.7 in the first 200 min of leaching). The acid

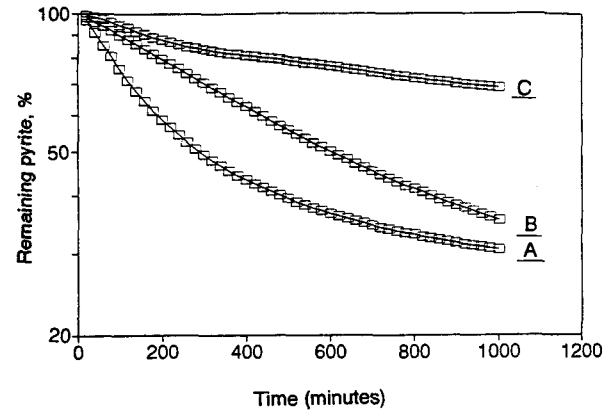


Figure 2. The first-order plot of $\log (100 \times M/M_0)$ versus t for the data of pyrite oxidation when pyrite was leached with the following three solutions: A, 0.147 mol/L H_2O_2 ; B, 0.147 mol/L H_2O_2 plus 0.013 mol/L EDTA; C, 0.147 mol/L H_2O_2 plus 0.01 mol/L KH_2PO_4 .

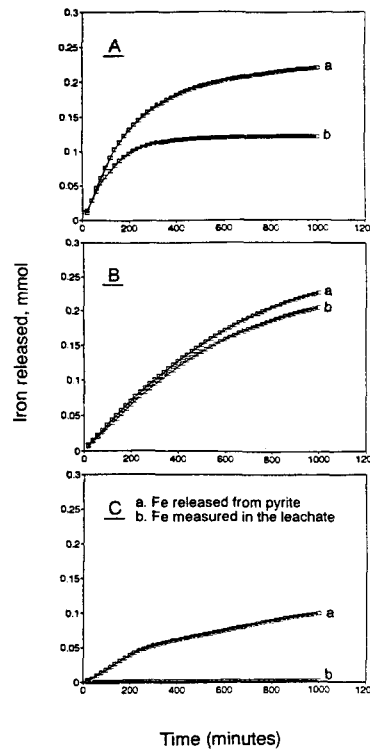


Figure 3. Release of iron as calculated according to the $Fe-SO_4$ stoichiometry and as measured in the leachates when pyrite was leached with the solutions listed in figure 2.

can inhibit formation of iron phosphate coatings owing to its influence on the degree of supersaturation with respect to FePO_4 and thereby increase the amount of pyrite oxidized to create iron phosphate coatings. The use of a buffer reagent will greatly decrease the amount of pyrite oxidized to create the coating.

Surface Analysis

Scanning electron microscope photos show that after leaching with 0.147 mol/L H_2O_2 , the residual pyrite particles were coated with a layer of iron hydroxide. But the framboidal morphology of most pyrite particles were still distinguishable (fig. 6A). This indicates that iron hydroxide did not precipitate as a coating owing to its relatively high solubility, although 0.1 mol of iron hydroxide formed during leaching within the column. As expected, the residual pyrite particles leached with the solution containing 0.147 mol/L H_2O_2 and 0.013 mol/L EDTA were free of any coatings (fig. 6B). Most pyrite particles displayed a typical framboidal morphology. Nevertheless, after leaching with the solution containing 0.147 mol/L H_2O_2 and 0.01 mol/L KH_2PO_4 , residual pyrite particles were so heavily coated with FePO_4 that crystals constituting pyrite particles were barely identifiable (fig. 6C). In addition, pyrite particles were much smaller than was observed for residual pyrite particles after leaching with H_2O_2 or H_2O_2 plus EDTA. This indicates that leaching with the phosphate solution containing H_2O_2 will introduce an iron phosphate coating on any size of pyrite particles.

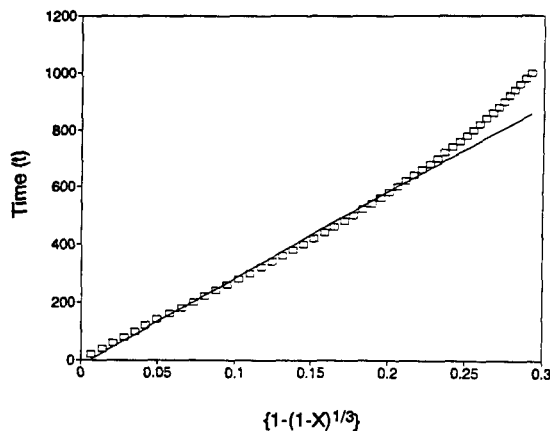


Figure 4. A model plot of t versus $\{1-(1-X)^{1/3}\}$ for the data of pyrite oxidation during leaching with the solution containing 0.147 mol/L H_2O_2 and 0.013 mol/L EDTA.

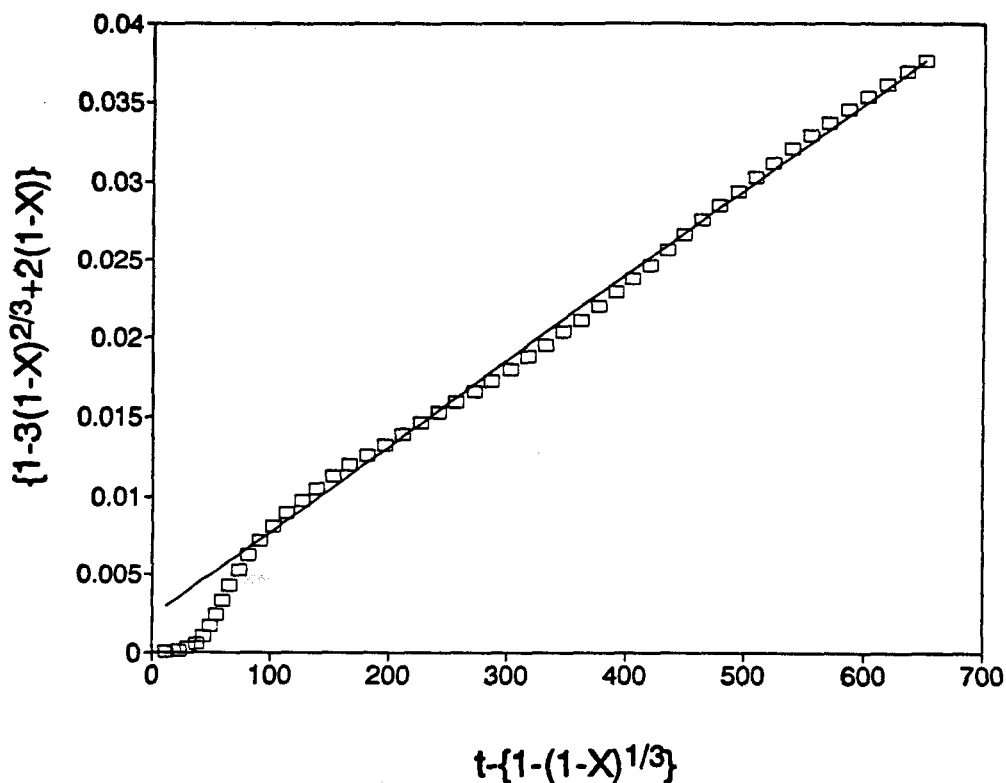


Figure 5. A model plot of $\{1-3(1-X)^{2/3}+2(1-X)\}$ versus $t-\{1-(1-X)^{1/3}\}$ for the data of pyrite oxidation during leaching with the solution containing 0.147 mol/L H_2O_2 and 0.01 mol/L KH_2PO_4 .

101

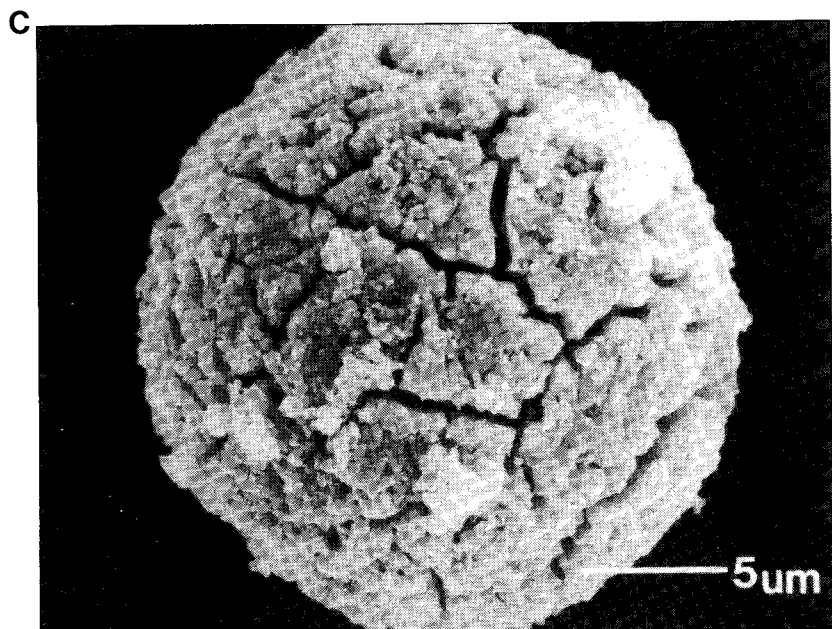
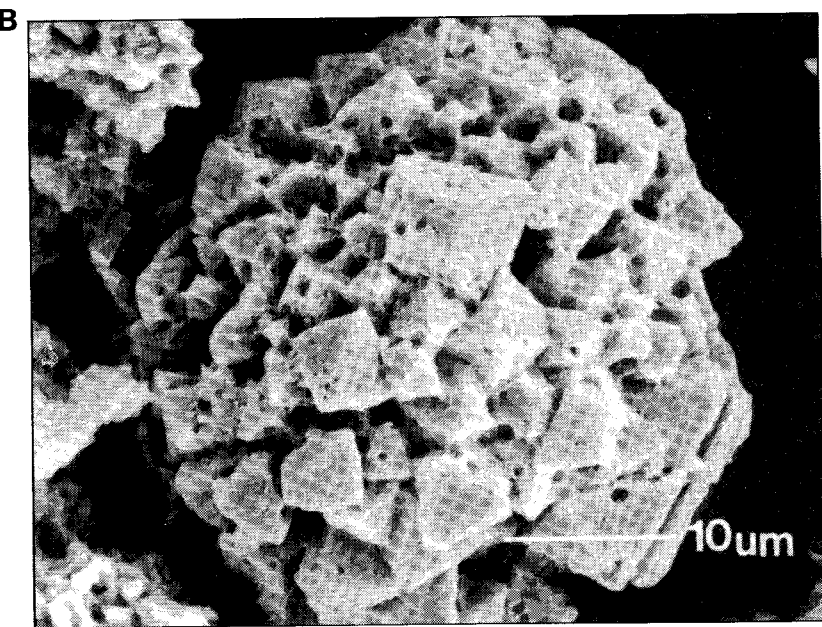
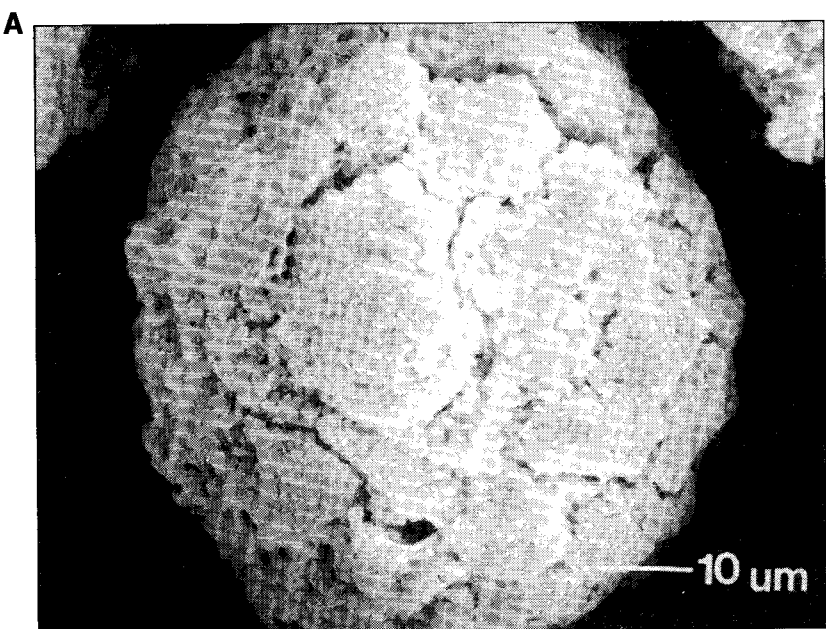


Figure 6. Scanning electron microscope photos showing the surface status of pyrite particles after leaching with A, 0.147 mol/L H_2O_2 ; B, 0.147 mol/L H_2O_2 plus 0.013 mol/L EDTA; C, 0.147 mol/L H_2O_2 plus 0.01 mol/L KH_2PO_4 .

Considering an FePO_4 precipitate of 0.1 mol with an FePO_4 gravity density of 2.73 g cm^{-3} and a pyrite specific surface of $7.3 \text{ m}^2/\text{g}$, its thickness was estimated to be approximately 188 \AA (assuming that all the iron phosphate was precipitated as coating). Although the coating appears to be thin, the results in figure 2 indicate that once the coating was established H_2O_2 in the coating solution could no longer attack pyrite, and that iron phosphate coating was an effective H_2O_2 -diffusion inhibitor.

To further understand the chemical properties of the iron phosphate coating, we repeated the leaching experiment with two columns of pure pyrite (50 mg pyrite and 500 mg sand) and the solution containing $0.147 \text{ mol/L H}_2\text{O}_2$ and $0.01 \text{ mol/L KH}_2\text{PO}_4$. At the end of leaching, one column continued to be leached with 50 mL of 2 mol/L HCl . The leachate was analyzed for iron and phosphate. We found out that the mole ratio of iron to phosphate was 1.0, indicating that the coating was FePO_4 and no hydroxyl entered the structure of iron phosphate. The pyrite in the other column was separated from the pyrite-sand mixture and its surface was examined using diffuse reflectance infrared spectroscopy (FT-IR). As shown in figure 7 (curve A), after leaching with the solution containing $0.147 \text{ mol/L H}_2\text{O}_2$ and $10^{-2} \text{ mol/L KH}_2\text{PO}_4$, the intensity of the IR absorption band at 439.7 cm^{-1} on the spectrum of the pyrite dramatically decreased. This absorption band was due to the vibration of the disulfide (S-S) in the lattice of pyrite; the decrease in intensity of this band strongly confirms the presence of the coating on pyritic surfaces. Three additional bands at 1624.3 , 1184.7 , and 1156.7 cm^{-1} and a broad band ranging from 3700 to 2800 cm^{-1} were also observed on the spectrum of the FePO_4 -coated pyrite (Fig. 7A). The absorption band at 1624 cm^{-1} and the absorption hump around 3000 cm^{-1} are attributable to the bending vibration and rotation of water molecules either adsorbed on iron phosphate or within the structure of iron phosphate. The adsorption bands at 1184.7 and 1156.6 cm^{-1} are due to the P-O internal stretching vibration of PO_4 group (Nanzyo, 1986). Comparison of the spectra of FePO_4 -coated pyrite and amorphous iron phosphate indicates that the iron phosphate coating is most likely amorphous material (Fig. 7A and 7C). However, the slight splitting of the P-O stretching vibration band at 1168 cm^{-1} suggests the tendency of iron phosphate coatings to become crystalline.

Effectiveness of the FePO_4 Coating in Preventing Pyrite Oxidation

We further tested the feasibility of this coating approach in preventing pyrite oxidation with the pulverized pyritic shale (the sample from which the pure framboidal pyrite was separated). We first leached the shale sample (500 mg) with 500 mL of a solution containing $0.053 \text{ mol/L H}_2\text{O}_2$ and $10^{-4} \text{ mol/L KH}_2\text{PO}_4$. This coating process consumed approximately 10% of the total amount of pyrite in the pyritic shale. The pyritic shale was then subjected to leaching with $0.088 \text{ mol/L H}_2\text{O}_2$ to test the effectiveness of the coating in preventing pyrite oxidation. As shown in figure 8, after leaching with $0.088 \text{ mol/L H}_2\text{O}_2$ for 800 min, only 15% of pyrite in the coated pyritic shale was oxidized, as opposed to more than 80% of pyrite oxidized in the uncoated pyritic shale. This result strongly suggests that the iron phosphate coatings can effectively protect pyrite from oxidizing.

Conclusions

The results of this study demonstrate that an amorphous iron phosphate coating can be established on the surfaces of pyrite in mining "waste" by leaching with a phosphate solution containing H_2O_2 and that the iron phosphate coating could

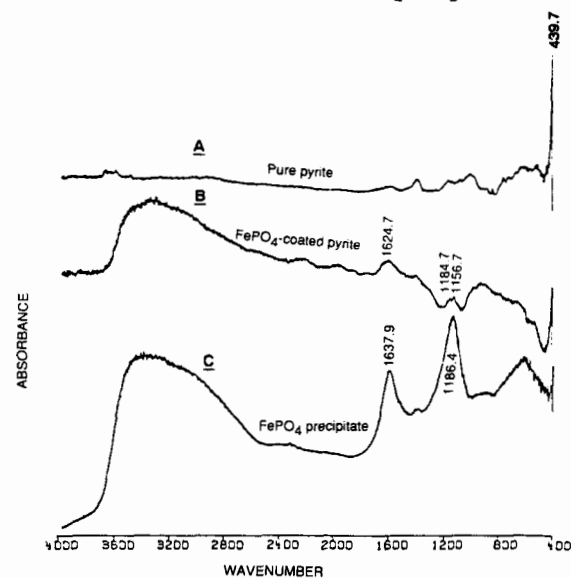


Figure 7. Infrared spectra of A, pyrite; B, FePO_4 -coated pyrite and C, FePO_4 precipitate.

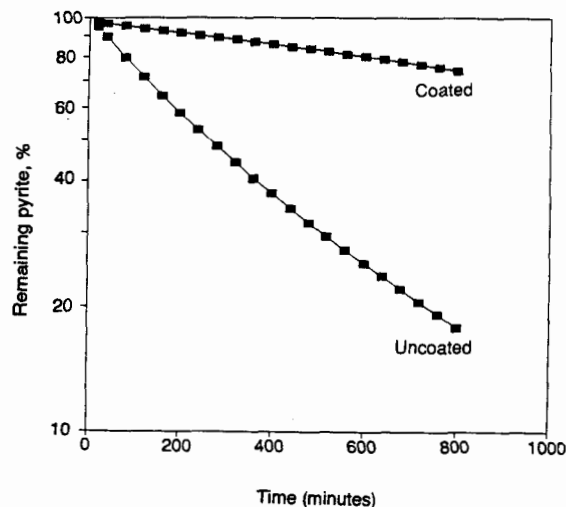


Figure 8. The plot of $\log (100 \times M/M_0)$ versus t for the data of pyrite oxidation when the uncoated and coated pyritic shale samples were leached with $0.088 \text{ mol/L H}_2\text{O}_2$.

effectively prevent pyrite oxidation.

The above conclusion sheds light on a possible solution to the long-unsolved problem of acid mine drainage. This coating approach or technology, if finally extended into practical use, has the following advantages over other approaches. First, due to the permanence of iron phosphate coatings on pyritic surfaces, pyrite particles in mining "waste" can no longer be oxidized and release acid; thus the prevention of the production of acid mine drainage could be permanent. Second, this coating approach does not require the physical mixing of coal wastes with ameliorants and thus can greatly simplify the operation. Third, the coating approach involves using only low concentrations of phosphate and hydrogen peroxide and can dramatically decrease the costs incurred in the operation.

The conclusions drawn in this study are mainly based on the small column experiments, where the effect of the acid produced during leaching with the coating solution on formation of iron phosphate coatings was minimized. It is expected that if we use the coating solution to leach large piles of coal "waste," the pH and concentrations of H₂O₂ and phosphate will decrease as the coating solution goes through the coal wastes. It has been proven in our laboratory that decreases in concentrations of H₂O₂ and phosphate will not significantly influence the efficiency of the coating solution. Nevertheless, the decrease in pH can pose a severe problem; when the pH of the coating solution drops below 4 or to 2, the solution no longer serves as a coating solution but becomes an oxidizing solution. Therefore, it seems essential to introduce a buffer in the coating solution to maintain the pH and the efficiency of the coating solution. Currently, in our laboratory, we are developing a coating solution with an optimal concentration combination of H₂O₂, KH₂PO₄, and a buffer reagent to prevent coal wastes from producing acid drainage.

Literature Cited

- Singer, P.C. and W. Stumm. 1970. Acid mine drainage: the rate-determining step Science 167:1121-1123.
- Silverman, M.P. 1967. Mechanisms of bacterial pyrite oxidation J. Bacteriology 94:1046-1051
- Nordstrom, D.K. 1982. Aqueous pyrite oxidation and the consequent formation of secondary iron minerals. p. 46-53. In L.R. Hossner, J.A. Kittrick, and D.F. Fanning (eds.), Acid sulfate weathering: pedogeochimistry and relationship to manipulation of soil minerals, Soil Sci. Soc. America, Madison, WI.
- Kleinmann, R.L.P., D.A. Crerar, and R.R. Pacelli. 1981 Biogeochemistry of acid mine drainage and a method to control acid formation Min. Eng. 3:300-305.
- Ziemkiewicz, P. 1990. Advances in the prediction of and control of acid mine drainage. p. 51-54. In Proceedings of the Mining and Reclamation Conference and Exhibition, v 2. Charleston, WV.
- Ivanov, V.I. 1962. Effect of some factors on iron oxidation by cultures of *Thiobacillus ferrooxidans*. Microbiology (Engl. Transl.) 31:645-648.
- Kleinmann, R.L.P., and D.A. Crerar, 1979. *Thiobacillus Ferrooxidans* and the formation of acidity in simulated coal mine environments. Geomicrobiology J. 1:373-389.
- Huang, X and V.P. Evangelou. 1992. Abatement of acid mine drainage by encapsulation of acid producing geologic materials. U.S. Bur. Mines Contract j0309013. 60 p.
- Nicholson, R. V., R. W. Gillham, and E. J. Reardon. 1989. Pyrite oxidation in carbonate-buffered solution: 2. Rate control by oxide coatings. Geochim. Cosmochim. Acta 54:395-402.
- Turner, R.C. 1960. An investigation of the intercept method for determining the proportion of dolomite and calcite in the mixtures of two. Can. J. Soil Sci. 40:232-241.
- Nanzyo, M. 1986. Infrared spectra of phosphate sorbed on iron hydroxide gel and the sorption products. Soil Sci. Plant Nutri. 32:51-58.